

000 001 002 003 004 005 006 007 008 009 010 011 012 013 014 015 016 017 018 019 020 021 022 023 024 025 026 027 028 029 030 031 032 033 034 035 036 037 038 039 040 041 042 043 044 045 046 047 048 049 050 051 052 053 SOLVING THE GRANULARITY MISMATCH: HIERARCHICAL PREFERENCE LEARNING FOR LONG- HORIZON LLM AGENTS

Anonymous authors

Paper under double-blind review

ABSTRACT

Large Language Models (LLMs) as autonomous agents are increasingly tasked with solving complex, long-horizon problems. Aligning these agents via **preference-based methods** like Direct Preference Optimization (DPO) is a promising direction, yet it faces a critical granularity mismatch. **Trajectory-level DPO provides stable signals but blur where credit should be assigned within long trajectories, whereas step-level DPO offers fine-grained supervision but can be statistically noisy and data-inefficient when Monte Carlo rollouts are limited, and can be hard to fully exploit multi-step structured behaviors that only reveal their effect over several actions.** To balance this trade-off, we introduce **Hierarchical Preference Learning (HPL)**, a hierarchical framework that optimizes LLM agents by leveraging preference signals at multiple, complementary granularities. While HPL incorporates trajectory- and step-level DPO for global and local policy stability, its core innovation lies in group-level preference optimization guided by a dual-layer curriculum. HPL first decomposes expert trajectories into semantically coherent action groups and then generates contrasting suboptimal groups to enable preference learning at a fine-grained, sub-task level. Then, instead of treating all preference pairs equally, HPL introduces a curriculum scheduler that organizes the learning process from simple to complex. This curriculum is structured along two axes: the group length, representing sub-task complexity, and the sample difficulty, defined by the reward gap between preferred and dispreferred action groups. Experiments on three challenging agent benchmarks show that HPL outperforms existing state-of-the-art methods. Our analyses demonstrate that the hierarchical DPO loss effectively integrates preference signals across multiple granularities, while the dual-layer curriculum is crucial for enabling the agent to solve a wide range of tasks, from simple behaviors to complex multi-step sequences.

1 INTRODUCTION

Large Language Models (LLMs) have evolved from static question-answering systems into autonomous agents capable of perceiving, reasoning, and acting within complex, open-ended environments (Li et al., 2024; Gou et al., 2025). This transformation has powered a new generation of applications, from embodied assistants that navigate simulated homes (Shridhar et al., 2021) to web navigators that execute multi-step online tasks (Zheng et al., 2024; Furuta et al., 2024). Unlike single-turn tasks, these agent-environment interactions unfold in multi-turn loops over extended periods (Wang et al., 2024a). This paradigm shift introduces a core challenge: long-horizon planning and decision-making, where the agent must execute a coherent sequence of actions to succeed.

To equip agents for such tasks, Reinforcement Learning (RL) has become a crucial recipe for post-training LLMs (Liu et al., 2024). Online RL methods like PPO (Sutton et al., 1998; Schulman et al., 2017) often entail substantial computational costs, high sample inefficiency, and risky, inefficient exploration in vast action spaces. **These challenges have motivated approaches that reduce reliance on online interaction by learning from static datasets collected in advance.** Direct Preference Optimization (DPO) (Rafailov et al., 2023) directly aligns agent policies using preference pairs (*e.g.*, expert vs. suboptimal behaviors) without requiring costly environment interaction or an explicitly trained reward model.

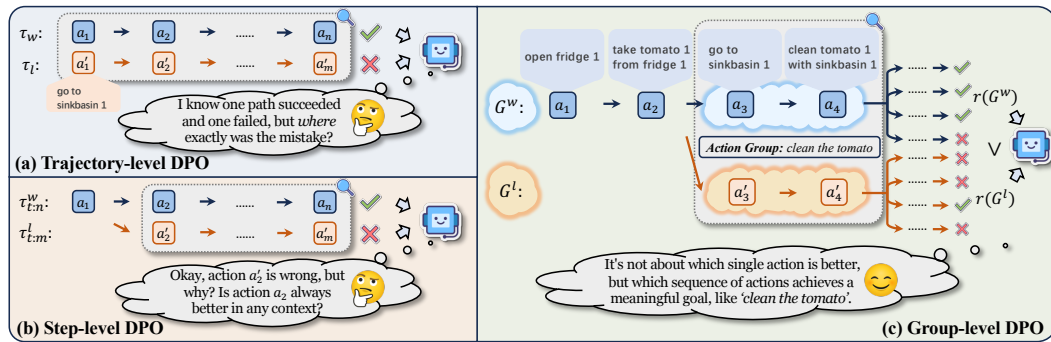


Figure 1: Conceptual comparison of different DPO granularities. While (a) trajectory-level DPO provides a coarse but stable signal and (b) step-level DPO offers focused but potentially noisy supervision, (c) our proposed Group-level DPO learns from semantically coherent action groups, which provides a structured signal, enabling the agent to reason at the sub-task level.

However, applying DPO to long-horizon agent tasks reveals a fundamental challenge we term the **granularity mismatch**. On one hand, trajectory-level DPO, such as ETO (Song et al., 2024), compares entire trajectories and yields stable, low-variance feedback aligned with final outcomes, but it provides limited resolution for credit assignment, which is hard to tell which segment of a long interaction actually determined success or failure. On the other hand, step-level DPO, employed by methods such as IPR (Xiong et al., 2024), attributes preferences to individual decisions by estimating the expected return from each decision point via Monte Carlo rollouts. However, this fine-grained focus poses practical challenges in the finite-data, limited-rollout regime. Supervision becomes fragmented across many decision points, so each step is updated from only a few noisy rollouts, and it can be hard to fully exploit multi-step structured behaviors whose contribution to success only becomes apparent when several actions are considered jointly. For instance, the sub-task of “retrieving an apple from the fridge” is composed of a chain of actions—navigating, opening, and taking—whose collective value cannot be captured by rewarding any single action in isolation.

To resolve this dilemma, we introduce **Hierarchical Preference Learning** (HPL), a hierarchical framework that optimizes LLM agents by leveraging preference signals at multiple, synergistic granularities. HPL first addresses the granularity mismatch by incorporating DPO losses at the trajectory, action, and the action-group levels. The group-level view provides both a **structural prior** by focusing supervision on sub-trajectories that are more likely to encode reusable skills and a **statistical benefit** by aggregating the contribution of multiple actions into one decision unit, which reduces variance relative to per-step Monte Carlo estimates under a fixed rollout budget. Beyond merely combining these losses, the core innovation of HPL is a dual-layer curriculum learning strategy that guides the training process. This curriculum systematically organizes the learning path from simple to complex along two orthogonal axes: sub-task complexity, defined by the length of an action group, and sample difficulty, measured by the reward gap between preferred and dispreferred behaviors. By first mastering simple, easily distinguishable sub-tasks, the agent builds a foundation before progressing to more complex challenges.

Our main contributions are summarized as follows:

- We identify and address the granularity mismatch problem in **preference-based** agent alignment by proposing a novel hierarchical framework that integrates preference signals at three distinct levels: the coarse trajectory-level, the fine-grained step-level, and a intermediate action-group level.
- We introduce HPL, a novel training paradigm with a dual-layer curriculum learning strategy. This is the first work to apply a structured curriculum to action-group level preference optimization, dynamically scheduling samples based on both task complexity and distinguishability.
- We design and systematically evaluate a range of action grouping strategies, from simple heuristics to a semantic-based approach, to generate meaningful sub-tasks for our framework.
- We demonstrate through extensive experiments on three diverse and challenging long-horizon benchmarks that HPL significantly outperforms existing state-of-the-art methods, establishing a more effective and principled paradigm for **preference-based training of LLM agents from fixed datasets after a one-shot exploration phase**.

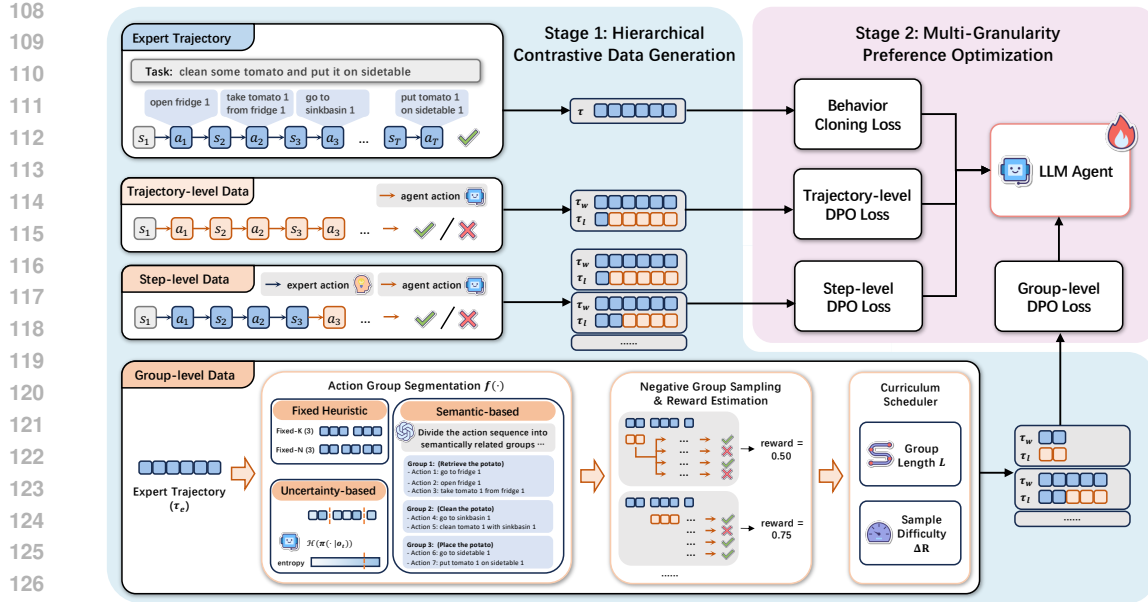


Figure 2: An overview of our proposed framework, HPL. Stage 1 generates hierarchical preference data with Action Group Segmentation component. Stage 2 then optimizes the agent with a composite objective, where the training is guided by dual-layer curriculum scheduler.

2 RELATED WORK

LLM-based Agents. The remarkable reasoning and instruction-following capabilities of modern LLMs have enabled their use as autonomous agents capable of tackling complex, interactive tasks (Li et al., 2024; Gou et al., 2025). Initial approaches primarily leveraged the in-context learning abilities of LLMs through prompts like ReAct (Yao et al., 2023) and Reflexion (Shinn et al., 2023) to elicit multi-step reasoning and action generation. To enhance the performance of open-source models beyond zero-shot prompting, a subsequent line of work has focused on fine-tuning agents on collected trajectory data (Chen et al., 2023). These methods range from standard Supervised Fine-Tuning (SFT) on expert demonstrations (Zeng et al., 2023; Chen et al., 2024) to more advanced techniques that learn from preference data, such as contrasting successful and failed trajectories to optimize for final outcomes (Song et al., 2024). While effective, these fine-tuning paradigms often treat entire trajectories as monolithic data points (Wang et al., 2024b), overlooking the fine-grained procedural knowledge embedded within the interaction trajectory.

Process Supervision. To address the limitations of outcome-based rewards, particularly the challenge of credit assignment in long-horizon tasks, a growing body of research has explored process supervision (Luo et al., 2024; Xiong et al., 2025). The core idea is to provide agents with more granular feedback at intermediate steps of a task. Early efforts in this area often relied on costly human annotations to label the correctness of each step (Lightman et al., 2023). To automate this, recent methods have proposed various techniques to estimate step-level rewards, such as using Monte Carlo rollouts to predict the future outcome from an intermediate state (Xiong et al., 2024) or training a separate reward model to predict the value of each action (Choudhury, 2025; Wang et al., 2025). These approaches typically use the estimated step-level rewards to guide the agent via reinforcement learning (Feng et al., 2025; Zhang et al., 2025) or DPO at the single-action level.

3 METHODOLOGY

In this section, we present our novel agent alignment framework **Hierarchical Preference Learning** (HPL) as depicted in Figure 2. We detail the principal phases of our method below: initial policy bootstrapping through behavior cloning, the generation of multi-granularity preference data, the design of our dual-layer curriculum scheduler, and finally, the hierarchical optimization objective.

162
163

3.1 PROBLEM SETTING

164
165

In this work, HPL follow the same two-stage protocol as previous work (Song et al., 2024; Xiong et al., 2024) that combines a one-shot exploration phase with purely offline preference optimization.

166

- **Fixed exploration and labeling.** A frozen reference policy π_{ref} interacts with the environment once to collect a pool of interaction traces, including both full trajectories and partial segments. We then run Monte Carlo rollouts with π_{ref} on this static pool to derive different level reward estimates, constructing the preference datasets. Importantly, the policy π_{θ} is never updated during this phase, and no further data collection is performed once the datasets are built.

171
172
173

- **Offline preference optimization.** Given these fixed datasets, preference-based methods train the target policy π_{θ} using DPO-style objectives at different levels (trajectory, step, and group), without any additional environment interaction or reward queries.

174
175
176
177

We therefore view our setting as offline preference optimization after a one-shot exploration phase, which is distinct from fully online RL methods such as PPO (Schulman et al., 2017) that continuously interleave policy updates with new environment rollouts throughout training.

178
179

3.2 BOOTSTRAPPING VIA EXPERT BEHAVIOR CLONING

180
181
182
183
184
185

To equip the base model with fundamental task-solving capabilities, we perform behavior cloning on a dataset of expert trajectories $\mathcal{D}_{\text{expert}} = \{(u, \tau^*)^{(i)}\}_{i=1}^{|\mathcal{D}_{\text{expert}}|}$, where u is the task instruction and τ^* is the corresponding expert trajectory. Each trajectory τ is a sequence of alternating states and actions $\tau = (s_1, a_1, s_2, a_2, \dots, s_T, a_T)$. A state s_t is a textual description of the environment, and an action a_t is a textual command generated by the agent. This process aims to maximize the likelihood of the expert's actions. The loss is defined as:

186
187
188
189

$$\mathcal{L}_{\text{BC}}(\theta; \mathcal{D}_{\text{expert}}) = -\mathbb{E}_{(u, \tau^*) \sim \mathcal{D}_{\text{expert}}} \left[\sum_{t=1}^{|\tau^*|} \log \pi_{\theta}(a_t^* | s_t^*, u, \tau_{<t}^*) \right], \quad (1)$$

190
191
192

where $\tau_{<t}^*$ represents the history $(s_1^*, a_1^*, \dots, s_{t-1}^*, a_{t-1}^*)$. This initial cloning step yields a competent base agent, which serves as our reference policy π_{ref} for the subsequent optimization stages.

193
194

3.3 HIERARCHICAL CONTRASTIVE DATA GENERATION

195
196
197
198
199

After obtaining a competent reference policy π_{ref} via behavior cloning (Section 3.2), the next stage is to generate a rich, multi-layered dataset for preference optimization. This is achieved by having π_{ref} interact with the environment to produce a diverse set of suboptimal trajectories. By contrasting these with expert trajectories, we construct three distinct preference datasets at the trajectory, action, and group granularities, as illustrated in the left panel of Figure 2.

200
201

3.3.1 DATA GENERATION AT TRAJECTORY AND ACTION LEVELS

202
203
204
205

Trajectory-Level Data. This dataset provides a coarse, outcome-based learning signal. For each expert trajectory τ_w from $\mathcal{D}_{\text{expert}}$, we use π_{ref} to generate a corresponding full trajectory τ_l . If the outcome reward of τ_l is lower than that of τ_w , we form a preference pair (τ_w, τ_l) . This process yields a trajectory-level dataset $\mathcal{D}_{\text{traj}} = \{(u, \tau_w, \tau_l)^{(i)}\}$, where u is the task instruction.

206
207
208
209
210
211
212

Step-Level Data. To provide a finer-grained, process-oriented signal, we adopt the methodology from IPR (Xiong et al., 2024). At each step t of an expert trajectory, we use the history $\tau_{<t}$ as a prompt for our reference agent π_{ref} to generate an alternative action \hat{a}_t and complete the rest of the trajectory, yielding $\tau_{t:m}^l$. This is contrasted with the expert's subsequent trajectory $\tau_{t:n}^w$. This creates a preference pair conditioned on the shared history, resulting in a step-level preference dataset $\mathcal{D}_{\text{step}} = \{(\tau_{<t}, \tau_{t:n}^w, \tau_{t:m}^l)^{(i)}\}$.

213
214
215

3.3.2 GROUP-LEVEL DATA GENERATION VIA ACTION GROUP SEGMENTATION

To bridge the gap between coarse trajectories and single actions, we introduce the core concept of an **action group**. These groups serve as an intermediate unit of reasoning, ideally corresponding to

216 semantically coherent sub-tasks for more effective credit assignment. The generation of group-level
 217 data involves two key steps: segmenting trajectories into groups and then estimating a quantitative
 218 reward for each group.

219 First, we apply a segmentation function $f(\cdot)$ to partition expert trajectory τ_w into corresponding
 220 action groups $\{G_{w,i}\}_{i=1}^N$. We design and investigate four distinct segmentation strategies:

222 **Fixed Heuristic Strategies.** As baselines, we consider two straightforward methods based on
 223 length. *Fixed-N Groups* divides a trajectory into a fixed number N of equal-length groups. *Fixed-K*
 224 *Size* creates groups with K consecutive action steps each. While simple, these methods are agnostic
 225 to the task’s semantic structure and risk making arbitrary cuts.

226 **Uncertainty-Based Segmentation.** This adaptive strategy is based on the intuition that a policy’s
 227 uncertainty often increases at sub-task boundaries (Guo et al., 2025). We leverage the entropy of
 228 the reference policy’s action distribution, $H(\pi_{\text{ref}}(\cdot|o_t))$, as a proxy for uncertainty. A boundary is
 229 inserted after action a_{t-1} if the entropy at step t exceeds a predefined threshold ϵ .

230 **Semantic Segmentation.** To achieve the most meaningful partitions, we employ a powerful, pre-
 231 trained LLM (e.g., GPT-4o) as an off-the-shelf “semantic segmenter”. We provide the full text
 232 transcript of a trajectory to the model and prompt it to partition the sequence into high-level sub-
 233 tasks based on their apparent goals (e.g., “find an object”, “operate an appliance”). This method is
 234 expected to yield the highest quality segmentations.

235 Once an expert trajectory is partitioned into a sequence of winning groups $\{G_{w,i}\}$, we construct
 236 the preference pairs required for our group-level optimization. For each expert action group $G_{w,i}$,
 237 which begins from a context c_i (i.e., the history of all preceding steps), we generate a corresponding
 238 losing group $G_{l,i}$. This is achieved by sampling a new action sequence of the same length from
 239 the reference policy $\pi_{\text{ref}}(\cdot|c_i)$. This length-constrained sampling ensures a fair, apples-to-apples
 240 comparison between the expert and suboptimal behaviors. The resulting tuples $(c_i, G_{w,i}, G_{l,i})$ form
 241 a rich dataset of fine-grained preference pairs, which are the fundamental training units for HPL.

242 3.3.3 GROUP-LEVEL REWARD ESTIMATION

244 After segmenting trajectories into groups, we need a quantitative reward estimate for each group to
 245 filter data and enable our curriculum learning strategy (detailed in Section 3.4). We define the reward
 246 of an action group G_i , which ends at timestep t_i with history $\tau_{<t_i}$, as the expected final outcome
 247 reward of trajectories completed from that point. Given the difficulty of direct computation, we
 248 estimate this value using Monte Carlo (MC) sampling. Specifically, we use our reference policy π_{ref}
 249 to perform M stochastic rollouts starting from the state after G_i has been executed. The estimated
 250 reward for the action group G_i , denoted $\hat{r}(G_i)$, is the average of the final outcome rewards $R(\cdot)$
 251 from these rollouts:

$$252 \hat{r}(G_i) = \frac{1}{M} \sum_{j=1}^M R(\tau_i^{(j)}), \quad \text{where } \{\tau_i^{(j)}\}_{j=1}^M = \text{MC}^{\pi_{\text{ref}}}(\tau_{<t_i}; M). \quad (2)$$

254 This MC estimation is applied to every winning group $G_{w,i}$ and losing group $G_{l,i}$ to obtain their
 255 rewards. With these components, we finalize our group-level dataset $\mathcal{D}_{\text{group}} = \{(c, G_w, G_l)^{(i)}\}$,
 256 where each entry contains a context, a preference pair of groups, and their estimated rewards.

257 **While step-level MC estimation provides a principled, localized estimate of the expected return**
 258 **at each decision point, in practice the rollout budget per state is small. Under this limited-rollout**
 259 **regime, per-step estimates can have high variance, which makes purely step-level preference learning**
 260 **statistically inefficient. In contrast, our group-level rewards aggregate the outcomes of multiple**
 261 **actions into a single supervision unit, amortizing the same rollout budget over longer sub-trajectories**
 262 **and better capturing their joint contribution to task success.**

264 3.4 DUAL-LAYER CURRICULUM LEARNING

266 Statically mixing the group-level preference data from all difficulties for training can be suboptimal,
 267 as it may expose the model to highly complex samples before it has developed foundational skills,
 268 leading to unstable or inefficient learning. To address this, we introduce the core innovation of our
 269 framework: a **dual-layer curriculum learning** strategy. This strategy dynamically organizes the
 training process to mimic an efficient human learning path, from simple concepts to complex ones.

270
 271 **The 2D Curriculum Matrix.** As illustrated in Figure 3, our curriculum is conceptualized as a two-
 272 dimensional difficulty matrix. We categorize each
 273 group-level preference pair (G_w, G_l) along two or-
 274 thogonal axes:

275 • **Sub-task Complexity (Y-axis):** This dimension is
 276 measured by the **Group Length** (L). Shorter ac-
 277 tion groups (e.g., 1-3 steps) correspond to simple,
 278 fundamental skills, while longer groups represent
 279 more complex, multi-step behaviors that require
 280 longer-term planning.
 281 • **Sample Discriminability (X-axis):** This dimen-
 282 sion is measured by the **Sample Difficulty** (ΔR),
 283 defined as the difference between the estimated re-
 284 wards of the winning and losing groups: $\Delta R =$
 285 $\hat{r}(G_w) - \hat{r}(G_l)$. A large ΔR indicates an easy-
 286 to-distinguish sample where the losing group is
 287 clearly inferior. A small ΔR represents a hard-to-
 288 distinguish sample that requires finer judgment from
 289 the agent for successful policy refinement.

290 Based on these two axes, we partition the group-level dataset $\mathcal{D}_{\text{group}}$ into a 3×3 grid of data buckets,
 291 denoted as $\mathcal{B}_{L,D}$, where $L, D \in \{1, 2, 3\}$ represent the levels of length and difficulty, respectively.

292 **The Curriculum Schedule.** Our training process is not a single pass over the mixed data, but
 293 a staged schedule that progressively expands the training set, guiding the model along a path of
 294 increasing difficulty. The schedule consists of three distinct phases:

295 1. **Phase 1 (Foundational Skills):** Initially, the model is trained exclusively on the easiest data
 296 bucket, $\mathcal{B}_{1,1}$ (short length, easy difficulty). This allows the agent to quickly and stably learn the
 297 most fundamental and unambiguous skills without being distracted by more complex scenarios.
 298 2. **Phase 2 (Expanding Complexity):** After the initial phase, we expand the training data to include
 299 $\mathcal{B}_{1,1} \cup \mathcal{B}_{1,2} \cup \mathcal{B}_{2,1}$. In this stage, the agent begins to tackle harder (less distinguishable) short-
 300 horizon tasks while also being introduced to simple medium-horizon skills, effectively broadening
 301 its capabilities.
 302 3. **Phase 3 (Full-Scale Tuning):** Finally, the training set is expanded to include all nine buckets
 303 $(\bigcup_{L,D} \mathcal{B}_{L,D})$. The agent now fine-tunes its policy on the full spectrum of complexities and
 304 difficulties, mastering the most challenging and nuanced aspects of the tasks.

305 This staged exposure ensures a smooth learning gradient, building agent’s expertise from the ground
 306 up and preventing it from being overwhelmed by difficult samples early in the training process.

308 3.5 MULTI-GRANULARITY PREFERENCE OPTIMIZATION

310 In the final stage, we optimize the policy π_θ using a composite loss function that integrates signals
 311 from all three granularities. This approach ensures that the agent not only learns from high-level
 312 outcomes and fine-grained sub-tasks but also stays grounded in the expert’s behavior. The final loss
 313 includes a sum of three components:

314 **Trajectory-Level DPO Loss ($\mathcal{L}_{\text{traj-DPO}}$).** To learn from the overall outcome, we apply a DPO loss
 315 on the trajectory-level dataset $\mathcal{D}_{\text{traj}}$. This loss encourages the policy to assign a higher likelihood to
 316 the entire successful trajectory over the failed one:

$$317 \mathcal{L}_{\text{traj-DPO}}(\theta; \mathcal{D}_{\text{traj}}) = -\mathbb{E}_{(\tau_w, \tau_l) \sim \mathcal{D}_{\text{traj}}} \left[\log \sigma \left(\beta \log \frac{\pi_\theta(\tau_w|u)}{\pi_{\text{ref}}(\tau_w|u)} - \beta \log \frac{\pi_\theta(\tau_l|u)}{\pi_{\text{ref}}(\tau_l|u)} \right) \right]. \quad (3)$$

320 **Step-Level DPO Loss ($\mathcal{L}_{\text{step-DPO}}$).** Drawing from Xiong et al. (2024), this loss uses $\mathcal{D}_{\text{step}}$ to provide
 321 step-level supervision by comparing the entire future from a decision point:

$$322 \mathcal{L}_{\text{step-DPO}}(\theta; \mathcal{D}_{\text{step}}) = -\mathbb{E}_{(\tau_{}, \tau_{t:n}^w, \tau_{t:m}^l) \sim \mathcal{D}_{\text{step}}} \left[\log \sigma \left(\beta \log \frac{\pi_\theta(\tau_{t:n}^w | \tau_{})}{\pi_{\text{ref}}(\tau_{t:n}^w | \tau_{})} - \beta \log \frac{\pi_\theta(\tau_{t:m}^l | \tau_{})}{\pi_{\text{ref}}(\tau_{t:m}^l | \tau_{})} \right) \right]. \quad (4)$$

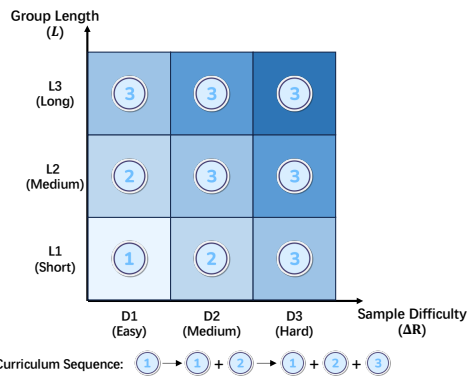


Figure 3: Illustration of the dual-layer curriculum scheduler with group length (L) and sample difficulty (ΔR). The training follows a three-phase schedule.

324 **Group-Level DPO Loss ($\mathcal{L}_{\text{group-DPO}}$).** This is the core component of our framework, providing mid-
 325 level supervision. We apply the DPO loss to the group-level dataset $\mathcal{D}_{\text{group}}$, comparing corresponding
 326 action groups:

$$327 \quad \mathcal{L}_{\text{group-DPO}}(\theta; \mathcal{D}_{\text{group}}) = -\mathbb{E}_{(c, G_w, G_l) \sim \mathcal{D}_{\text{group}}} \left[\log \sigma \left(\beta \log \frac{\pi_\theta(G_w|c)}{\pi_{\text{ref}}(G_w|c)} - \beta \log \frac{\pi_\theta(G_l|c)}{\pi_{\text{ref}}(G_l|c)} \right) \right]. \quad (5)$$

330 We briefly analyze the bias-variance properties of this group-level objective in the following propo-
 331 sition, with a full derivation provided in Appendix F.

332 **Proposition 1** (Bias-variance trade-off of group-level DPO loss). *Let T denote the trajectory length,
 333 $\gamma \in [0, 1)$ the discount factor, and R_{\max} the maximum reward. Let $\mathcal{L}_{\text{traj}}$, $\mathcal{L}_{\text{step}}$, and $\mathcal{L}_{\text{group}}(k)$ denote
 334 the empirical losses of trajectory-level, step-level, and group-level DPO with group length $k < T$,
 335 respectively. Then there exists a constant $C > 0$ depending only on $(\gamma, \pi_{\text{ref}})$ such that for every
 336 $\epsilon \in (0, 1)$ the choice $k(\epsilon) = \lceil \log_\gamma \left(\frac{(1-\gamma)\epsilon}{2\beta R_{\max}} \right) \rceil$ satisfies*

$$338 \quad \text{Bias}(\mathcal{L}_{\text{group}}(k)) \leq \min\{\text{Bias}(\mathcal{L}_{\text{traj}}), \text{Bias}(\mathcal{L}_{\text{step}})\} + \epsilon, \quad (6)$$

$$340 \quad \text{Var}(\mathcal{L}_{\text{group}}(k)) \leq \frac{C \log(1/\epsilon)}{T} \min\{\text{Var}(\mathcal{L}_{\text{traj}}), \text{Var}(\mathcal{L}_{\text{step}})\}. \quad (7)$$

342 Hence, by setting $k = \Theta(\log(1/\epsilon))$, group-level DPO loss simultaneously improves the variance by
 343 a factor $\Omega(T/\log(1/\epsilon))$ while incurring at most an additive bias of ϵ over the other two losses.

344 The final training objective combines these losses:

$$346 \quad \mathcal{L}_{\text{final}}^{(s)} = \mathcal{L}_{\text{BC}} + \mathcal{L}_{\text{traj-DPO}} + \mathcal{L}_{\text{step-DPO}} + \mathcal{L}_{\text{group-DPO}}^{(s)}, \quad (8)$$

348 where the group-level loss $\mathcal{L}_{\text{group-DPO}}^{(s)}$ for curriculum stage s is computed over a dynamically selected
 349 subset of data, $\mathcal{D}_{\text{group}}^{(s)}$, which is determined by our curriculum scheduler (Section 3.4). The data
 350 subset $\mathcal{D}_{\text{group}}^{(s)}$ for each stage is constructed from the 2D curriculum matrix buckets $\mathcal{B}_{L,D}$ as follows:

$$353 \quad \mathcal{D}_{\text{group}}^{(s)} = \begin{cases} \mathcal{B}_{1,1} & \text{if } s = 1 \text{ (Phase 1)} \\ \mathcal{B}_{1,1} \cup \mathcal{B}_{1,2} \cup \mathcal{B}_{2,1} & \text{if } s = 2 \text{ (Phase 2)} \\ \bigcup_{L,D} \mathcal{B}_{L,D} & \text{if } s = 3 \text{ (Phase 3)} \end{cases} \quad (9)$$

357 4 EXPERIMENTS

359 In this section, we conduct a series of experiments to comprehensively evaluate the performance of
 360 our HPL framework. Our evaluation is designed to answer the following key research questions:

362 **RQ1.** Does HPL outperform strong baselines that rely on conventional learning granularities,
 363 such as the trajectory-level (ETO) and step-level (IPR)?

364 **RQ2.** What is the impact of different action group segmentation strategies on the final perfor-
 365 mance of the agent?

366 **RQ3.** How crucial is the dual-layer curriculum mechanism to the success of HPL, and what is
 367 the contribution of each curriculum layer?

368 **RQ4.** How do trajectory-level, step-level, and group-level losses contribute to HPL?

370 4.1 EXPERIMENTAL SETUP

372 We evaluate our proposed method, HPL, on three diverse and challenging long-horizon agent bench-
 373 marks: ALFWorld (Shridhar et al., 2021), WebShop (Yao et al., 2022), and InterCode-SQL (Yang
 374 et al., 2023). In all our benchmarks, the environment returns a single terminal outcome reward at
 375 the end of each episode, which defines a finite-horizon episodic MDP and can be modeled with γ
 376 close to 1 and suitably rescaled rewards. For all experiments, we use Qwen2.5-1.5B-Instruct and
 377 Qwen2.5-7B-Instruct as the backbone language models. HPL is compared against a suite of strong
 378 baselines, including SFT, RFT (Yuan et al., 2023), ETO (Song et al., 2024), and IPR (Xiong et al.,

378 Table 1: Performance comparison of HPL and baselines across agent benchmarks **over 3 random**
 379 **seeds**. All methods are evaluated using Qwen2.5-1.5B-Instruct and Qwen2.5-7B-Instruct as base
 380 models. The best and second-best results are highlighted in **bold** and with an underline, respectively.
 381

382 Models	383 ALFWorld		384 WebShop		385 InterCode-SQL		386 Average
	387 seen	388 unseen	389 avg. reward	390 success rate	391 avg. reward	392 success rate	
GPT-4o	36.43	32.09	55.26	18.50	28.50	28.50	33.21
Gemini-2.5-Pro	55.71	49.25	49.56	19.50	68.42	66.00	51.40
Qwen2.5-1.5B-Instruct	2.14	0.00	36.09	10.50	5.50	5.50	9.95
SFT	60.95 ± 1.09	57.96 ± 1.88	56.56 ± 0.69	26.00 ± 0.50	56.24 ± 0.61	54.33 ± 0.76	52.01 ± 0.43
RFT (Yuan et al., 2023)	61.19 ± 1.80	60.95 ± 0.86	57.66 ± 1.45	28.17 ± 1.04	58.08 ± 0.64	56.67 ± 0.29	53.79 ± 0.40
ETO (Song et al., 2024)	65.48 ± 3.60	66.42 ± 2.24	56.57 ± 0.22	28.00 ± 0.87	58.45 ± 1.01	57.67 ± 0.76	55.43 ± 0.86
IPR (Xiong et al., 2024)	65.24 ± 2.30	66.67 ± 3.68	57.76 ± 1.13	27.83 ± 1.04	58.26 ± 1.78	57.17 ± 1.04	55.49 ± 0.78
HPL (Fixed-N (3))	69.52 ± 1.48	74.38 ± 1.14	60.21 ± 2.04	30.17 ± 1.61	58.75 ± 0.67	57.67 ± 0.58	58.45 ± 0.60
HPL (Fixed-K (3))	70.48 ± 1.09	66.42 ± 2.69	58.34 ± 1.84	28.33 ± 0.58	<u>59.69 ± 0.58</u>	57.17 ± 0.76	56.74 ± 0.79
HPL (Uncertainty)	74.53 ± 2.89	64.18 ± 1.29	58.75 ± 0.55	27.83 ± 0.76	59.11 ± 0.66	57.33 ± 0.29	56.95 ± 0.44
HPL (Semantic)	72.86 ± 1.89	74.13 ± 1.88	60.74 ± 1.08	30.00 ± 1.00	60.39 ± 0.74	58.50 ± 1.00	59.44 ± 0.63
Qwen2.5-7B-Instruct	38.57	45.52	56.61	19.50	8.80	8.50	29.58
SFT	67.62 ± 2.18	73.63 ± 3.11	60.64 ± 1.12	31.83 ± 1.26	66.70 ± 1.11	65.17 ± 0.76	60.93 ± 0.71
RFT (Yuan et al., 2023)	71.43 ± 1.89	72.63 ± 3.02	61.16 ± 0.85	33.50 ± 1.00	68.01 ± 0.89	66.33 ± 0.76	62.18 ± 0.11
ETO (Song et al., 2024)	72.62 ± 2.51	77.86 ± 2.40	61.85 ± 1.00	33.17 ± 1.04	68.32 ± 0.86	67.00 ± 0.50	63.47 ± 0.47
IPR (Xiong et al., 2024)	73.10 ± 1.80	78.11 ± 3.76	62.01 ± 0.43	33.67 ± 0.58	68.86 ± 1.02	67.17 ± 0.58	63.82 ± 0.69
HPL (Fixed-N (3))	78.33 ± 2.51	78.86 ± 2.40	62.11 ± 0.41	34.33 ± 0.76	69.55 ± 1.38	68.00 ± 1.00	65.20 ± 0.38
HPL (Fixed-K (3))	85.71 ± 2.58	78.61 ± 1.55	62.01 ± 1.04	33.83 ± 1.26	69.40 ± 0.98	68.17 ± 0.58	66.29 ± 0.54
HPL (Uncertainty)	83.10 ± 1.80	83.33 ± 1.88	62.79 ± 0.85	35.33 ± 1.04	69.21 ± 0.47	67.83 ± 0.29	66.93 ± 0.43
HPL (Semantic)	82.62 ± 2.30	84.08 ± 2.28	62.97 ± 0.50	35.17 ± 0.58	70.37 ± 1.27	68.50 ± 1.32	67.28 ± 0.47

400 2024). All methods are initialized from an SFT model trained on expert trajectories generated by
 401 a GPT-4o teacher model. For MC estimation, we use $M = 5$ rollouts for per group. For Fixed- N
 402 and Fixed- K strategy, we set $N = 3$ and $K = 3$. For Uncertainty strategy, the entropy thresh-
 403 old ϵ is set to the 80th percentile of all action entropies (*i.e.*, the threshold for the top 20% highest
 404 values) computed across the training dataset. Detailed descriptions of the environments, baseline
 405 implementations, and all hyperparameters are deferred to Appendix C.

4.2 MAIN RESULTS (RQ1, RQ2)

409 As shown in Table 1, our HPL framework outperforms all baseline methods across both model
 410 scales, providing a clear answer to our first research question. For the Qwen2.5-7B-Instruct model,
 411 our best-performing variant, HPL (Semantic), achieves an average score of 67.28, surpassing the
 412 strongest single-granularity baselines, ETO and IPR, by 3.81 and 3.46 points, respectively, and
 413 maintaining this advantage across all three benchmarks. The benefit of HPL’s hierarchical
 414 approach is especially notable in tasks requiring complex, long-horizon generalization: on ALFWorld
 415 unseen scenarios, HPL (Semantic) attains a mean success rate of 84.08%, nearly 6 points higher
 416 than state-of-the-art IPR (78.11%). These results indicate that by integrating preference signals at
 417 the trajectory, action, and group levels, HPL effectively resolves the granularity mismatch problem
 418 and learns a more robust and generalizable policy.

419 Our experiments also reveal the critical impact of the action group segmentation strategy, directly
 420 addressing our second research question. While all HPL variants consistently outperform the base-
 421 lines, adaptive, content-aware segmentation methods generally yield better performance than heuris-
 422 tic approaches. In particular, HPL (Semantic), which partitions trajectories into semantically coher-
 423 ent sub-tasks, is the top-performing variant for both the 1.5B and 7B models, outpacing the next-
 424 best HPL (Uncertainty) by over 0.35 point in mean average score on the 7B model. This suggests
 425 that the quality of the action groups is paramount: providing the DPO loss with more meaningful,
 426 human-aligned sub-tasks as comparison units leads to a more effective learning signal. Moreover,
 427 the strong performance of the simpler Uncertainty and Fixed-N strategies demonstrates the value of
 428 incorporating an intermediate granularity, validating the core design of our framework.

4.3 ANALYSIS OF THE CURRICULUM LEARNING MECHANISM (RQ3)

431 **Ablation of Curriculum Components.** To quantitatively assess the importance of our dual-layer
 432 curriculum, we conduct an ablation study by removing each layer individually, with results presented

Table 2: Ablation study on our curriculum learning mechanism of HPL across three agent benchmarks.

Models	ALFWorld		WebShop		InterCode-SQL		Average
	seen	unseen	avg. reward	success rate	avg. reward	success rate	
Qwen2.5-1.5B-Instruct							
HPL	71.43	72.39	59.99	30.00	60.08	58.50	58.73
HPL Static	68.57	71.64	58.80	29.00	59.45	58.00	57.58
HPL Length CL Only	69.29	72.39	58.06	28.50	59.39	57.50	57.52
HPL Difficulty CL Only	71.43	70.71	58.83	30.00	60.50	58.00	58.25
Qwen2.5-7B-Instruct							
HPL	83.57	86.57	62.56	34.50	70.63	69.00	67.81
HPL Static	75.71	82.84	62.05	33.00	69.71	68.50	65.30
HPL Length CL Only	82.14	85.07	62.26	34.00	69.49	67.50	66.74
HPL Difficulty CL Only	81.43	85.82	62.27	34.50	69.63	68.00	66.94

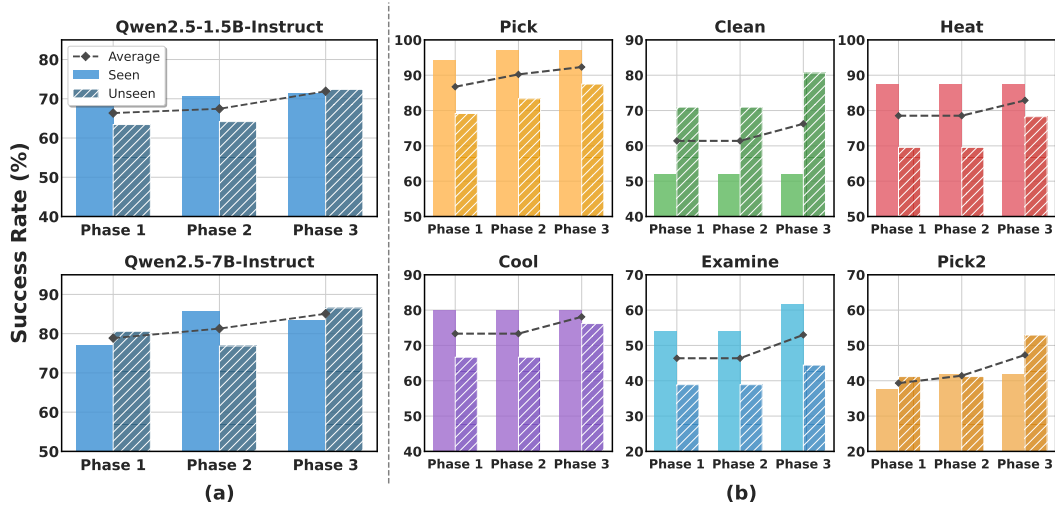


Figure 4: Phase-wise performance progression of HPL on the ALFWorld benchmark. (a) Success rates for both 1.5B and 7B models across the three curriculum phases. (b) A detailed breakdown for the 1.5B model on 6 sub-task types.

in Table 2. The primary finding is that the full HPL model, equipped with both curriculum layers, consistently outperforms all ablated variants. Removing the curriculum entirely (HPL Static) results in the most significant performance degradation across both model scales, confirming that employing a curriculum is crucial for effective learning. Furthermore, the results indicate that both the length and difficulty-based curricula contribute positively to the final performance, with their individual removal leading to noticeable performance drops. This demonstrates the synergistic benefit of our dual-layer design, where organizing the learning process first by task complexity (length) and then by solution quality (difficulty) provides a more effective path to mastering complex agent behaviors.

Phase-wise Performance Progression. To provide a more fine-grained view of how the curriculum works, Figure 4 visualizes the agent’s performance at the end of each curriculum phase. Panel (a) shows a clear improvement in the overall success rate for both the 1.5B and 7B models as they progress from Phase 1 to Phase 3. This trend holds for the unseen scenarios, indicating that the curriculum effectively helps the model generalize its learned skills. Panel (b) offers a deeper insight by breaking down the performance by sub-task type for the 1.5B model. We observe that while simpler tasks like Pick are learned relatively early, more complex tasks requiring longer reasoning chains, such as Clean and Pick2, show the most substantial performance gains in the later phases.

4.4 ABLATION ON HIERARCHICAL DPO LOSSES (RQ4)

To investigate the individual contribution of each component in our hierarchical framework, we conduct an ablation study on the three DPO losses, with results shown in Figure 5. The results reveal that while all three loss components, trajectory, action, and group, contribute positively to

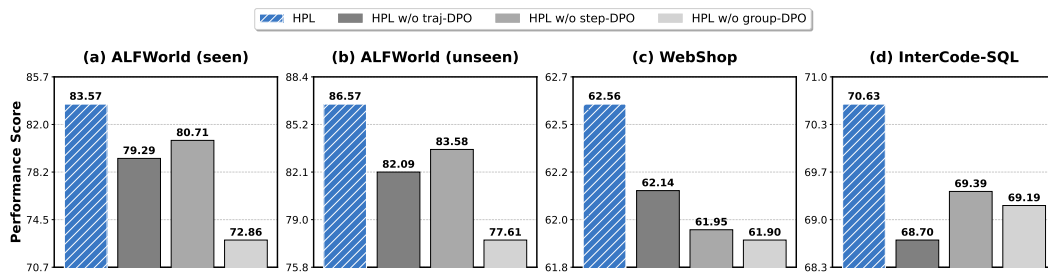


Figure 5: Ablation study on the HPL loss components on Qwen2.5-7B-Instruct.

the final performance, the group-level DPO is demonstrably the most critical. Across all benchmarks, removing the group-level signal (HPL w/o group-DPO) induces a significantly more severe performance degradation than removing either the trajectory or step-level signals. This provides compelling evidence that the action-group granularity is the primary driver of HPL’s effectiveness, serving as a crucial bridge between coarse trajectory feedback and action supervision and validating the synergistic benefit of our three-level approach.

5 DISCUSSION

In this section, we discuss why group-level objectives are effective for long-horizon LLM agents. Building on both our theoretical analysis and empirical ablations, we highlight two complementary perspectives: (i) segmentation introduces a useful **structural prior** over sub-tasks, and (ii) group-level objectives have favorable **statistical properties** in the finite-data, limited-rollout regime.

Segmentation as a structural prior. Group-level supervision implicitly encodes prior knowledge about long-horizon task structure: instead of treating every individual action as an equally important learning unit, it focuses the objective on short sub-trajectories that are more likely to correspond to meaningful sub-tasks. Although HPL reuses exactly the same interaction data as trajectory- and step-level baselines, reorganizing this data into action groups changes where supervision is concentrated. Empirical results show that the semantic variant using a stronger segmentation prior achieves the best overall performance, while simpler segmenters still improve over both trajectory and step-level DPO, despite having almost no semantic information about sub-task boundaries.

Statistical properties in the finite-data regime. From an asymptotic perspective, a sufficiently expressive step-level DPO objective could in principle represent the same long-horizon credit assignment as a group-level objective. Our focus, however, is the practically relevant regime where both the dataset size and the MC rollout budget per state are limited. Under this regime, step-level MC estimates provide localized but noisy supervision: each decision point is updated from only a small number of rollouts. Group-level objectives alleviate this by aggregating multiple actions into a single supervised unit. With the same overall rollout budget, group-level rewards effectively average out noise over longer sub-trajectories and directly evaluate the joint contribution of several actions to task success. Proposition 1 formalizes this intuition through a bias–variance analysis, and our ablation studies further show that removing the group-level loss significantly degrades performance.

6 CONCLUSION

In this work, we address the critical issue of granularity mismatch in preference-based alignment for LLM agents. We introduce Hierarchical Preference Learning (HPL), a novel framework that resolves this challenge by integrating preference signals across three levels of abstraction: trajectory, action, and a crucial, intermediate action-group level. By partitioning trajectories into semantically coherent sub-tasks and optimizing a hierarchical DPO loss, HPL learns to directly prefer successful multi-step action sequences over flawed alternatives. Extensive experiments demonstrate that HPL outperforms strong prior methods that operate primarily at the extreme granularities of entire trajectories or individual actions, across a suite of complex, long-horizon agent benchmarks. In conclusion, our work underscores the importance of learning from hierarchical signals that mirror the compositional nature of complex tasks, paving the way for more capable LLM agents.

540 REPRODUCIBILITY STATEMENT
541

542 Our experimental setup is briefly summarized in Section 4.1. To facilitate the reproduction of
543 our results, Appendix C offers a detailed account of all the benchmarks, data generation process,
544 baselines, and all hyperparameters. We also release the code and data, which are available at:
545 <https://anonymous.4open.science/r/HPL>.

547 REFERENCES
548

549 Baian Chen, Chang Shu, Ehsan Shareghi, Nigel Collier, Karthik Narasimhan, and Shunyu Yao.
550 Fireact: Toward language agent fine-tuning. *arXiv preprint arXiv:2310.05915*, 2023.

551 Zehui Chen, Kuikun Liu, Qiuchen Wang, Wenwei Zhang, Jiangning Liu, Dahua Lin, Kai Chen, and
552 Feng Zhao. Agent-flan: Designing data and methods of effective agent tuning for large language
553 models. *arXiv preprint arXiv:2403.12881*, 2024.

554 Sanjiban Choudhury. Process reward models for llm agents: Practical framework and directions.
555 *arXiv preprint arXiv:2502.10325*, 2025.

557 Lang Feng, Zhenghai Xue, Tingcong Liu, and Bo An. Group-in-group policy optimization for llm
558 agent training. *arXiv preprint arXiv:2505.10978*, 2025.

559 Hiroki Furuta, Kuang-Huei Lee, Ofir Nachum, Yutaka Matsuo, Aleksandra Faust, Shixiang Shane
560 Gu, and Izzeddin Gur. Multimodal web navigation with instruction-finetuned foundation models.
561 In *The Twelfth International Conference on Learning Representations*, 2024. URL <https://openreview.net/forum?id=effFmBWioSc>.

564 Boyu Gou, Ruohan Wang, Boyuan Zheng, Yanan Xie, Cheng Chang, Yiheng Shu, Huan Sun, and
565 Yu Su. Navigating the digital world as humans do: Universal visual grounding for GUI agents.
566 In *The Thirteenth International Conference on Learning Representations*, 2025. URL <https://openreview.net/forum?id=kxnoqaisCT>.

568 Yiran Guo, Lijie Xu, Jie Liu, Dan Ye, and Shuang Qiu. Segment policy optimization: Ef-
569 fective segment-level credit assignment in rl for large language models. *arXiv preprint*
570 *arXiv:2505.23564*, 2025.

571 Manling Li, Shiyu Zhao, Qineng Wang, Kangrui Wang, Yu Zhou, Sanjana Srivastava, Cem Gokmen,
572 Tony Lee, Erran Li Li, Ruohan Zhang, et al. Embodied agent interface: Benchmarking llms for
573 embodied decision making. *Advances in Neural Information Processing Systems*, 37:100428–
574 100534, 2024.

576 Hunter Lightman, Vineet Kosaraju, Yuri Burda, Harrison Edwards, Bowen Baker, Teddy Lee, Jan
577 Leike, John Schulman, Ilya Sutskever, and Karl Cobbe. Let’s verify step by step. In *The Twelfth*
578 *International Conference on Learning Representations*, 2023.

579 Aixin Liu, Bei Feng, Bing Xue, Bingxuan Wang, Bochao Wu, Chengda Lu, Chenggang Zhao,
580 Chengqi Deng, Chenyu Zhang, Chong Ruan, et al. Deepseek-v3 technical report. *arXiv preprint*
581 *arXiv:2412.19437*, 2024.

582 Liangchen Luo, Yinxiao Liu, Rosanne Liu, Samrat Phatale, Meiqi Guo, Harsh Lara, Yunxuan Li,
583 Lei Shu, Yun Zhu, Lei Meng, et al. Improve mathematical reasoning in language models by
584 automated process supervision. *arXiv preprint arXiv:2406.06592*, 2024.

586 Rafael Rafailov, Archit Sharma, Eric Mitchell, Christopher D Manning, Stefano Ermon, and Chelsea
587 Finn. Direct preference optimization: Your language model is secretly a reward model. *Advances*
588 *in Neural Information Processing Systems*, 36:53728–53741, 2023.

589 John Schulman, Filip Wolski, Prafulla Dhariwal, Alec Radford, and Oleg Klimov. Proximal policy
590 optimization algorithms. *arXiv preprint arXiv:1707.06347*, 2017.

592 Noah Shinn, Federico Cassano, Ashwin Gopinath, Karthik Narasimhan, and Shunyu Yao. Reflexion:
593 Language agents with verbal reinforcement learning. *Advances in Neural Information Processing*
594 *Systems*, 36:8634–8652, 2023.

594 Mohit Shridhar, Xingdi Yuan, Marc-Alexandre Cote, Yonatan Bisk, Adam Trischler, and Matthew
 595 Hausknecht. Alfworld: Aligning text and embodied environments for interactive learning. In
 596 *International Conference on Learning Representations*, 2021. URL <https://openreview.net/forum?id=0IOX0YcCdTn>.

598 Yifan Song, Da Yin, Xiang Yue, Jie Huang, Sujian Li, and Bill Yuchen Lin. Trial and error:
 599 Exploration-based trajectory optimization of LLM agents. In *Proceedings of the 62nd Annual*
 600 *Meeting of the Association for Computational Linguistics (Volume 1: Long Papers)*, pp. 7584–
 601 7600. Association for Computational Linguistics, 2024.

602 Richard S Sutton, Andrew G Barto, et al. *Reinforcement learning: An introduction*, volume 1. MIT
 603 press Cambridge, 1998.

605 Hanlin Wang, Chak Tou Leong, Jiashuo Wang, Jian Wang, and Wenjie Li. Spa-rl: Reinforcing llm
 606 agents via stepwise progress attribution. *arXiv preprint arXiv:2505.20732*, 2025.

607 Lei Wang, Chen Ma, Xueyang Feng, Zeyu Zhang, Hao Yang, Jingsen Zhang, Zhiyuan Chen, Jiakai
 608 Tang, Xu Chen, Yankai Lin, et al. A survey on large language model based autonomous agents.
 609 *Frontiers of Computer Science*, 18(6):186345, 2024a.

610 Renxi Wang, Haonan Li, Xudong Han, Yixuan Zhang, and Timothy Baldwin. Learning from failure:
 611 Integrating negative examples when fine-tuning large language models as agents. *arXiv preprint*
 612 *arXiv:2402.11651*, 2024b.

614 Wei Xiong, Wenting Zhao, Weizhe Yuan, Olga Golovneva, Tong Zhang, Jason Weston, and Sain-
 615 bayar Sukhbaatar. Stepwiser: Stepwise generative judges for wiser reasoning. *arXiv preprint*
 616 *arXiv:2508.19229*, 2025.

617 Weimin Xiong, Yifan Song, Xutian Zhao, Wenhao Wu, Xun Wang, Ke Wang, Cheng Li, Wei Peng,
 618 and Sujian Li. Watch every step! LLM agent learning via iterative step-level process refinement.
 619 In *Proceedings of the 2024 Conference on Empirical Methods in Natural Language Processing*,
 620 pp. 1556–1572. Association for Computational Linguistics, 2024.

621 John Yang, Akshara Prabhakar, Karthik Narasimhan, and Shunyu Yao. Intercode: Standardizing
 622 and benchmarking interactive coding with execution feedback. *Advances in Neural Information*
 623 *Processing Systems*, 36:23826–23854, 2023.

624 Shunyu Yao, Howard Chen, John Yang, and Karthik Narasimhan. Webshop: Towards scalable
 625 real-world web interaction with grounded language agents. *Advances in Neural Information Pro-
 626 cessing Systems*, 35:20744–20757, 2022.

628 Shunyu Yao, Jeffrey Zhao, Dian Yu, Nan Du, Izhak Shafran, Karthik Narasimhan, and Yuan Cao.
 629 React: Synergizing reasoning and acting in language models. In *International Conference on*
 630 *Learning Representations (ICLR)*, 2023.

631 Tao Yu, Rui Zhang, Kai Yang, Michihiro Yasunaga, Dongxu Wang, Zifan Li, James Ma, Irene
 632 Li, Qingning Yao, Shanelle Roman, Zilin Zhang, and Dragomir Radev. Spider: A large-scale
 633 human-labeled dataset for complex and cross-domain semantic parsing and text-to-SQL task. In
 634 *Proceedings of the 2018 Conference on Empirical Methods in Natural Language Processing*, pp.
 635 3911–3921. Association for Computational Linguistics, 2018.

636 Zheng Yuan, Hongyi Yuan, Chengpeng Li, Guanting Dong, Keming Lu, Chuanqi Tan, Chang Zhou,
 637 and Jingren Zhou. Scaling relationship on learning mathematical reasoning with large language
 638 models. *arXiv preprint arXiv:2308.01825*, 2023.

639 Aohan Zeng, Mingdao Liu, Rui Lu, Bowen Wang, Xiao Liu, Yuxiao Dong, and Jie Tang. Agenttun-
 640 ing: Enabling generalized agent abilities for llms. *arXiv preprint arXiv:2310.12823*, 2023.

642 Guibin Zhang, Hejia Geng, Xiaohang Yu, Zhenfei Yin, Zaibin Zhang, Zelin Tan, Heng Zhou,
 643 Zhongzhi Li, Xiangyuan Xue, Yijiang Li, et al. The landscape of agentic reinforcement learning
 644 for llms: A survey. *arXiv preprint arXiv:2509.02547*, 2025.

645 Boyuan Zheng, Boyu Gou, Jihyung Kil, Huan Sun, and Yu Su. GPT-4V(ision) is a generalist web
 646 agent, if grounded. In *Proceedings of the 41st International Conference on Machine Learning*,
 647 volume 235 of *Proceedings of Machine Learning Research*, pp. 61349–61385. PMLR, 21–27 Jul
 2024. URL <https://proceedings.mlr.press/v235/zheng24e.html>.

648

A THE USE OF LLMs

649
650 In the preparation of this manuscript and the development of our codebase, we utilized LLMs to
651 assist in two primary capacities. We detail these uses below for full transparency:652
653

- **Writing and Editing Assistance:** We used LLM as a writing assistant to improve the grammar,
654 phrasing, and overall clarity of the manuscript. The authors directed all core ideas and claims, and
655 are fully responsible for the final wording, arguments, and content presented in this paper.
- **Code Implementation Support:** During the implementation of our experimental framework, an
656 LLM served as a coding assistant for tasks such as generating basic code and aiding in debugging.
657 The authors designed the overall software architecture, and all LLM-generated code was carefully
658 reviewed and adapted by the authors to ensure its correctness and functionality.

659660

B BROADER IMPACTS AND LIMITATIONS

661
662 **Broader Impacts.** Our work on Hierarchical Preference Learning (HPL) presents a more efficient
663 and effective paradigm for training capable autonomous agents from fixed datasets after a one-shot
664 exploration phase. Technologically, this reduces the reliance on costly and often unsafe online
665 exploration, making the development of sophisticated LLM agents more accessible and sustainable.
666 The ability to learn from the compositional structure of tasks via action groups could lead to more
667 reliable and predictable agents in real-world applications, from personalized assistants to complex
668 workflow automation. On a societal level, the deployment of more competent agents can enhance
669 productivity and assist with complex decision-making. However, as agent capabilities advance,
670 ensuring their alignment with human values becomes paramount. The preferences learned from
671 static datasets must be carefully curated to prevent the codification of biases or unintended behaviors.
672 Furthermore, the increasing autonomy of such agents necessitates continued research into robust
673 safety protocols, transparency, and ethical oversight to mitigate potential misuse and ensure these
674 powerful technologies are developed responsibly for the benefit of society.
675676 **Limitations.** While our HPL framework demonstrates significant performance gains, we acknowl-
677 edge several limitations that offer avenues for future research. Firstly, the effectiveness of HPL,
678 particularly the semantic variant, is contingent on the quality of the action group segmentation. Al-
679 though our experiments show that simple heuristics are beneficial, a suboptimal segmentation could
680 yield less meaningful sub-tasks and hinder the learning process. Secondly, our dual-layer curricu-
681 lum, while effective, introduces a new set of hyperparameters for defining task complexity and sam-
682 ple distinguishability, and the optimal configuration of this curriculum may be domain-specific and
683 require careful tuning. Finally, our current work relies on a powerful teacher model for generating
684 preference data, which means the agent’s policy may inherit biases from the teacher. Future re-
685 search could explore more robust, self-supervised segmentation techniques and investigate methods
686 for learning curricula directly from the data.687

C EXPERIMENTAL DETAILS

688

C.1 ENVIRONMENTS AND TASKS

689 We evaluate our framework on three challenging benchmarks that require long-horizon, multi-step
690 reasoning and interaction, representing a diverse set of agent tasks.
691692

C.1.1 ALFWORLD

693
694 ALFWORLD (Shridhar et al., 2021) is an embodied agent benchmark set in simulated household en-
695 vironments, uniquely designed to align abstract, text-based interactions with a visually rich, embod-
696 ied world. Agents must parse natural language instructions and perform a sequence of high-level
697 actions (e.g., `goto`, `take`, `clean`) to complete common household tasks, such as “put a clean
698 tomato on the sidetable”. The benchmark is structured into six distinct and compositional sub-task
699 categories: `Pick`, `Clean`, `Heat`, `Cool`, `Examine`, and `Pick2`. The dataset contains 3,553 sce-
700 narios for training. For evaluation, the test set is divided into a seen set of 140 scenarios to assess
701 in-distribution generalization within familiar room layouts, and a more challenging unseen set of

702 134 scenarios with novel task instances in unobserved environments to evaluate out-of-distribution
 703 generalization. For all tasks, the maximum number of interaction turns is set to 30.
 704

705 **C.1.2 WEBSHOP**
 706

707 WebShop (Yao et al., 2022) is a web-based simulation environment that tasks agents with navigating
 708 a realistic e-commerce website to find and purchase a product that matches a given instruction.
 709 The environment is notable for its scale and realism, featuring 1.18 million real-world products and
 710 over 12,000 crowd-sourced, natural language instructions. To succeed, an agent must interact with
 711 multiple types of web pages, including search, results, and item-detail pages, by issuing high-level
 712 actions, primarily “search [QUERY]” or “click [BUTTON]”. This process requires a combination
 713 of information retrieval skills to formulate effective search queries and long-horizon planning to
 714 navigate the site, compare items, and select the correct product options. The final reward is automatically
 715 calculated based on a heuristic that measures the attribute, option, and price match between
 716 the purchased item and the user’s instruction. The benchmark includes 200 test tasks. For all tasks,
 717 the maximum number of interaction turns is set to 10.
 718

719 **C.1.3 INTERCODE-SQL**
 720

721 InterCode-SQL (Yang et al., 2023) is an interactive environment designed to benchmark agent
 722 capabilities in complex data querying tasks. Within a safe and reproducible Docker container, the
 723 agent interacts with a live MySQL database by iteratively writing and executing SQL queries to
 724 answer natural language questions. The environment is built upon the challenging, cross-domain
 725 Spider dataset (Yu et al., 2018), which requires the agent to understand complex database schemas
 726 and formulate queries that often involve multiple tables and JOIN operations. A key feature of this
 727 benchmark is its interactive nature; after each query execution, the agent receives real-world feed-
 728 back, such as query results or error messages, which it must use to debug and refine its subsequent
 729 actions. A final reward is calculated based on the Intersection over Union (IoU) between the agent’s
 730 submitted query results and the ground-truth records. The benchmark consists of 200 test tasks. For
 731 all tasks, the maximum number of interaction turns is set to 10.
 732

733 **C.2 MODELS AND IMPLEMENTATION DETAILS**
 734

735 Our methodology relies on a dataset of expert trajectories and generating a corresponding set of
 736 suboptimal trajectories for creating preference pairs.
 737

738 **Expert Trajectories ($\mathcal{D}_{\text{expert}}$).** Following prior work (Xiong et al., 2024), we generate our initial
 739 set of expert trajectories by prompting a powerful teacher model (GPT-4o) to solve tasks in each
 740 environment using a ReAct-style reasoning process. We then filter these generated trajectories,
 741 retaining only those that achieve a high outcome reward (*e.g.*, success score of 1.0 in ALFWorld and
 742 InterCode-SQL, or >0.8 in WebShop) to form our final expert dataset, $\mathcal{D}_{\text{expert}}$. This dataset is used
 743 for the initial behavior cloning stage.

744 **Models and Training.** We utilize Qwen2.5-1.5B-Instruct and Qwen2.5-7B-Instruct as the back-
 745 bone models for all experiments. For all DPO-based methods, including our HPL, the reference
 746 policy π_{ref} is the SFT agent trained on $\mathcal{D}_{\text{expert}}$. During the behavior cloning phase, models are
 747 trained for 3 epochs using the AdamW optimizer with a cosine learning rate schedule, peaking at
 748 1e-5. All experiments were conducted on 8 NVIDIA A800 80G GPUs.
 749

750 **C.3 BASELINES**
 751

752 We compare HPL against a suite of strong baselines representing different alignment strategies,
 753 ranging from standard imitation learning to state-of-the-art preference optimization methods.
 754

- 755 • **SFT:** The standard Supervised Fine-Tuning approach, where the model is trained only on
 756 the expert trajectories $\mathcal{D}_{\text{expert}}$. This serves as our foundational base model and represents
 757 the standard behavior cloning paradigm from which all other preference-based methods are
 758 initialized.

- **RFT** (Yuan et al., 2023): Rejection sampling Fine-Tuning is an enhanced fine-tuning method that uses rejection sampling to augment the expert dataset with newly generated successful trajectories. By enriching the training data with a more diverse set of successful paths, RFT serves as a strong imitation learning baseline that tests the performance limits of learning solely from positive demonstrations.
- **ETO** (Song et al., 2024): A trajectory-level DPO baseline that learns by contrasting full successful and failed trajectories. This method represents the coarsest end of the preference learning spectrum, providing a holistic signal based on the final outcome. While powerful, this approach faces challenges in credit assignment, as it can struggle to pinpoint specific errors within long action sequences.
- **IPR** (Xiong et al., 2024): A state-of-the-art process supervision method that performs step-level DPO using rewards estimated from Monte Carlo rollouts. IPR operates at the finest granularity, providing precise, localized feedback on individual actions. However, this step-level focus may overlook the synergistic value of multi-step sub-tasks.

C.4 HYPERPARAMETERS

Table 3 and Table 4 show the hyperparameters for SFT and Group-DPO stage respectively across three agent benchmarks. All experiments were conducted on 8 NVIDIA A800 80G GPUs.

Table 3: Hyperparamenters for SFT stage across three agent benchmarks.

Benchmark	ALFWorld	WebShop	InterCode-SQL
Batch size	32	32	32
Learning rate	1e-5	1e-5	1e-5
Optimizer	AdamW	AdamW	AdamW
LR scheduler	cosine	cosine	cosine
Warmup ratio	0.1	0.1	0.1
Max epochs	3	3	3
Max seq length	6000	6000	6000
DeepSpeed Zero stage	3	3	3
Gradient accumulation steps	2	2	2

Table 4: Hyperparamenters for Group-DPO stage across three agent benchmarks.

Benchmark	ALFWorld	WebShop	InterCode-SQL
Batch size	32	32	32
Learning rate	3e-6	1e-6	1e-6
β	0.3	0.3	0.3
Optimizer	AdamW	AdamW	AdamW
LR scheduler	cosine	cosine	cosine
Warmup ratio	0.1	0.1	0.1
Max epochs	1	1	1
Max seq length	6000	6000	6000
DeepSpeed Zero stage	3	3	3
Group length (L) threshold for curriculum	(0,3,6)	(0,2,4)	(0,2,4)
Difficulty (ΔR) threshold for curriculum	(1.0, 0.7, 0.4)	(1.0, 0.7, 0.4)	(1.0, 0.7, 0.4)

C.5 RESOURCE COMPARISON

We report in Table 5 a resource comparison of SFT, ETO, IPR, and the HPL variants on ALFWorld with Qwen2.5-1.5B-Instruct, including whether an external powerful LLM is used, the number of LLM calls, and the generation/training time.

During data generation, we adopt the same parallel sampling implementation provided by the ETO and IPR codebases to accelerate environment interaction. The actual generation time depends primarily on the degree of parallelism in environment rollouts, as well as the time required to reset the

810 Table 5: Resource comparison of SFT, ETO, IPR, and HPL variants on the ALFWorld benchmark
 811 with Qwen2.5-1.5B-Instruct.

813 Method	814 External powerful LLM	815 # LLM calls	816 Gen time	817 Train time
SFT	✗	0	0	18min
ETO	✗	~ 30,000	1h 7min	13min
IPR	✗	~ 750,000 (step-level part)	6h 13min (step-level part)	26min
HPL (Fixed-N(3))	✗	~ 207,000 (group-level part)	3h 35min (group-level part)	25min
HPL (Fixed-K(3))	✗	~ 213,000 (group-level part)	4h 15min (group-level part)	26min
HPL (Uncertainty)	✗	~ 194,000 (group-level part)	3h 47min (group-level part)	28min
HPL (Semantic)	✓	~ 221,000 (group-level part)	3h 21min (group-level part)	26min

820 environment and progress it to the desired states; the LLM call latency is not the dominant factor.
 821 The reported training times are based on real runs using 4 NVIDIA A800 80G GPUs.

823 D ILLUSTRATIVE EXAMPLE OF GROUP REWARD ESTIMATION

825 In this section, we provide a concrete walkthrough of how the Monte Carlo (MC) rollout mechanism
 826 estimates the expected outcome reward for a specific action group, as defined in Equation 2.

828 Consider an example from the ALFWorld benchmark:

- 829 • **Task Instruction:** put a clean apple in fridge
- 830 • **Current Context (c_i):** The agent is located at the sinkbasin 1 and is holding a dirty
 831 apple 1.
- 832 • **Candidate Action Group (G_i):** The policy generates a coherent sequence of actions in-
 833 tended to complete the “cleaning” sub-task:

$$834 G_i = [\text{go to sinkbasin 1, clean apple 1 with sinkbasin 1}]$$

836 To estimate the reward $\hat{r}(G_i)$, we first execute G_i . The simulation state transitions to a point where
 837 the agent is holding a *clean* apple at the sink. From this state, we perform $M = 3$ stochastic rollouts
 838 using the reference policy π_{ref} to see if the task can be successfully completed.

- 840 • **Rollout 1 ($\tau^{(1)}$):** The agent successfully navigates to the fridge, opens it, and places the
 841 apple inside.
 \rightarrow **Outcome Reward** $R(\tau^{(1)}) = 1.0$ (Success).
- 843 • **Rollout 2 ($\tau^{(2)}$):** The agent navigates to the fridge but attempts to place the apple without
 844 opening the fridge first. It fails to recover within the step limit.
 \rightarrow **Outcome Reward** $R(\tau^{(2)}) = 0.0$ (Failure).
- 846 • **Rollout 3 ($\tau^{(3)}$):** The agent navigates to the fridge, opens it, and successfully places the
 847 apple.
 \rightarrow **Outcome Reward** $R(\tau^{(3)}) = 1.0$ (Success).

850 Finally, the estimated reward for group G_i is calculated as the average of these outcomes:

$$852 \hat{r}(G_i) = \frac{1}{3}(1.0 + 0.0 + 1.0) \approx 0.67.$$

853 This value $\hat{r}(G_i) = 0.67$ serves as the quality label for this action group. If paired with a lower-
 854 quality group (e.g., one that failed to clean the apple), the difference ΔR determines the sample
 855 difficulty for our curriculum scheduler.

857 E DETAILS OF DUAL-LAYER CURRICULUM SCHEDULER

859 In this section, we provide the algorithmic implementation of our curriculum scheduler and a visual
 860 illustration of the phase-wise training progression.

862 Algorithm 1 outlines the logic for partitioning the preference data into the 3×3 grid based on Group
 863 Length (L) and Sample Difficulty (ΔR), and selecting the active data subsets for the current training
 864 phase s . We utilize the hyperparameters specified in Appendix C.4.

864 **Algorithm 1** HPL Dual-Layer Curriculum Scheduler

865 1: **Input:** Dataset \mathcal{D}_{all} , Phase $s \in \{1, 2, 3\}$, Thresholds $T_L, T_{\Delta R}$.

866 2: **Output:** Training subset $\mathcal{D}_{train}^{(s)}$.

867 3: **Step 1: Data Partitioning**

868 4: Partition \mathcal{D}_{all} into 3×3 buckets $\mathcal{B}_{l,d}$ where $l, d \in \{1, 2, 3\}$.

869 5: For each sample $x \in \mathcal{D}_{all}$, assign to $\mathcal{B}_{l,d}$ based on:

870 • Length Level l : Determined by group length vs. T_L (Short $\rightarrow 1$, Long $\rightarrow 3$).

871 • Difficulty Level d : Determined by reward gap vs. $T_{\Delta R}$ (Easy $\rightarrow 1$, Hard $\rightarrow 3$).

872 6: **Step 2: Phase-based Selection**

873 7: Define the set of active bucket indices $\mathcal{I}^{(s)}$ for current phase s :

874 8: **if** $s = 1$ **then**

875 9: $\mathcal{I}^{(1)} \leftarrow \{(1, 1)\}$ {Phase 1: Foundational (Short & Easy)}

876 10: **else if** $s = 2$ **then**

877 11: $\mathcal{I}^{(2)} \leftarrow \{(1, 1), (1, 2), (2, 1)\}$ {Phase 2: Expansion}

878 12: **else**

879 13: $\mathcal{I}^{(3)} \leftarrow \{(l, d) \mid 1 \leq l, d \leq 3\}$ {Phase 3: Full Scale}

880 14: **end if**

881 15: **return** $\mathcal{D}_{train}^{(s)} \leftarrow \bigcup_{(l,d) \in \mathcal{I}^{(s)}} \mathcal{B}_{l,d}$

882 **F ANALYSIS**

883

884 We now analyze the bias and variance of group-level DPO loss. Consider an MDP with discount
 885 factor $\gamma \in [0, 1)$. A trajectory τ of horizon T is denoted as $\tau = (s_1, a_1, r_1, \dots, s_T, a_T, r_T)$. Let
 886 π_{ref} be a reference policy strictly positive on every state-action pair. For any sequence u , we define
 887 its discounted return with respect to the (unknown) optimal value function V^* by

888

$$R(u) := \sum_{i \in u} \gamma^{i-t_0} r_i + \gamma^{|u|} V^*(s_{t_0+|u|}), \quad (10)$$

889

890 where t_0 is the starting time index of u and $|u|$ is its length. The true preference probability that u_w
 891 is preferred to u_l is modelled by the Bradley-Terry law

892

893

$$P(u_w \succ u_l) = \sigma \left(\beta \left[\log \frac{\pi^*(u_w)}{\pi_{\text{ref}}(u_w)} - \log \frac{\pi^*(u_l)}{\pi_{\text{ref}}(u_l)} \right] \right) := \sigma(\beta \Delta^*), \quad (11)$$

894

895 where $\sigma(z) = \frac{1}{1+e^{-z}}$ and $\beta > 0$ is a fixed inverse-temperature. The population DPO loss for a
 896 generic distribution μ over pairs (u_w, u_l) is

897

$$\mathcal{L}^\mu := -\mathbb{E}_\mu \log \sigma(\beta \Delta^*). \quad (12)$$

898

899 Given a dataset \mathcal{D} of N i.i.d. trajectories, each method forms its own empirical distribution μ_\bullet and
 900 minimizes

901

$$\mathcal{L}_\bullet(\theta; \mathcal{D}_\bullet) := -\frac{1}{|\mathcal{D}_\bullet|} \sum_{(u_w, u_l) \in \mathcal{D}_\bullet} \log \sigma(\beta \Delta_\theta), \quad (13)$$

902

903 where $\Delta_\theta := \log \frac{\pi_\theta(u_w)}{\pi_{\text{ref}}(u_w)} - \log \frac{\pi_\theta(u_l)}{\pi_{\text{ref}}(u_l)}$ and $\bullet \in \{\text{traj, step, group}\}$. We adopt the standard risk
 904 decomposition

905

$$\begin{aligned} \text{Risk}(\mathcal{L}_\bullet) &:= \mathbb{E}[(\mathcal{L}_\bullet - \mathcal{L}^{\mu_\bullet})^2] \\ &= \text{Bias}(\mathcal{L}_\bullet)^2 + \text{Var}(\mathcal{L}_\bullet), \end{aligned} \quad (14)$$

906

907 where the expectation $\mathbb{E}[\cdot]$ is taken over the sampling distribution of \mathcal{D}_\bullet and

908

909

$$\begin{aligned} \text{Bias}(\mathcal{L}_\bullet) &:= \mathbb{E}[\mathcal{L}_\bullet] - \mathcal{L}^{\mu_\bullet}, \\ \text{Var}(\mathcal{L}_\bullet) &:= \mathbb{E}[(\mathcal{L}_\bullet - \mathbb{E}[\mathcal{L}_\bullet])^2]. \end{aligned} \quad (15)$$

910

911 **Proposition 1** (Bias-variance trade-off of group-level DPO loss). *Let T denote the trajectory length,
 912 $\gamma \in [0, 1)$ the discount factor, and R_{\max} the maximum reward. Let $\mathcal{L}_{\text{traj}}$, $\mathcal{L}_{\text{step}}$, and $\mathcal{L}_{\text{group}}(k)$ denote
 913 the empirical losses of trajectory-level, step-level, and group-level DPO with group length $k < T$,*

918 respectively. Then there exists a constant $C > 0$ depending only on (γ, π_{ref}) such that for every
 919 $\epsilon \in (0, 1)$ the choice $k(\epsilon) = \lceil \log_\gamma \left(\frac{(1-\gamma)\epsilon}{2\beta R_{max}} \right) \rceil$ satisfies
 920

$$\text{Bias}(\mathcal{L}_{group}(k)) \leq \min\{\text{Bias}(\mathcal{L}_{traj}), \text{Bias}(\mathcal{L}_{step})\} + \epsilon, \quad (16)$$

$$\text{Var}(\mathcal{L}_{group}(k)) \leq \frac{C \log(1/\epsilon)}{T} \min\{\text{Var}(\mathcal{L}_{traj}), \text{Var}(\mathcal{L}_{step})\}. \quad (17)$$

925
 926 *Proof.* First, we analyze the bias of the three losses. We compare the population losses induced
 927 by the three sampling schemes. Recall that the logistic loss is 1-Lipschitz, that is, for any scalar
 928 difference z ,

$$|\log \sigma(z) - \log \sigma(z')| \leq |z - z'|. \quad (18)$$

929 Hence the bias of an empirical loss \mathcal{L}_\bullet is controlled by
 930

$$|\mathbb{E}[\mathcal{L}_\bullet] - \mathcal{L}^{\mu_\bullet}| \leq \beta \mathbb{E}_{\mu_\bullet} [|\Delta_\theta - \Delta^*|], \quad (19)$$

931 which is governed by the error in the return difference induced by the length of the comparison unit.
 932 We now analyze the three cases: trajectory, step, and group. Trajectory-level DPO compares entire
 933 trajectories with no truncation. Hence $\text{Bias}(\mathcal{L}_{traj}) = 0$. Step-level DPO compares suffixes from
 934 time t to T . Following the implementation in Xiong et al. (2024), these suffixes are not truncated
 935 either. Hence $\text{Bias}(\mathcal{L}_{step}) = 0$. For group-level DPO, the unit has fixed length $k < T$. For clarity,
 936 we define $R^*(t) := \sum_{i=t}^T \gamma^{i-t} r_i$. According to Bellman equation,
 937

$$R^*(t) = \sum_{i=t}^{t+k-1} \gamma^{i-t} r_i + \gamma^k R^*(t+k). \quad (20)$$

938 Consider a group pair (G_w, G_l) starting from the same state s_t , the true return difference should
 939 be $\delta_{traj} = R_w^*(t) - R_l^*(t)$, while group-level DPO uses $\delta_{group} = R(G_w) - R(G_l)$. Substituting
 940 Equation 20 into δ_{traj} , we get
 941

$$\delta_{traj} = \left[\sum_{i=t, r_i \in G_w}^{t+k-1} \gamma^{i-t} r_i + \gamma^k R_w^*(t+k) \right] - \left[\sum_{i=t, r_i \in G_l}^{t+k-1} \gamma^{i-t} r_i + \gamma^k R_l^*(t+k) \right] \quad (21)$$

$$= (R(G_w) - R(G_l)) + \gamma^k (R_w^*(t+k) - R_l^*(t+k)) \quad (22)$$

$$= \delta_{group} + \gamma^k (R_w^*(t+k) - R_l^*(t+k)). \quad (23)$$

942 Hence the error in the return difference is
 943

$$|\delta_{traj} - \delta_{group}| = \gamma^k |R_w^*(t+k) - R_l^*(t+k)| \leq \gamma^k \cdot \frac{2R_{max}}{1-\gamma}, \quad (24)$$

944 where the last step follows from the fact that the absolute value of any finite-horizon discounted sum
 945 is bounded by
 946

$$\sum_{i=t+k}^T \gamma^{i-(t+k)} |r_i| \leq R_{max} \sum_{j=0}^{T-(t+k)} \gamma^j < \frac{R_{max}}{1-\gamma}. \quad (25)$$

947 Therefore, for a single preference pair, the error of group-level DPO loss satisfies
 948

$$|\log \sigma(\beta \Delta_{group} - \log \sigma(\beta \Delta_{traj}))| \leq \beta |\Delta_{group} - \Delta_{true}| \leq \beta \cdot \frac{2R_{max}}{1-\gamma} \gamma^k. \quad (26)$$

949 Taking the expectation, we get
 950

$$\text{Bias}(\mathcal{L}_{group}) \leq \text{Bias}(\mathcal{L}_{traj}) + \frac{2\beta R_{max}}{1-\gamma} \gamma^k. \quad (27)$$

951 By choosing $k(\epsilon) = \lceil \log_\gamma \left(\frac{(1-\gamma)\epsilon}{2\beta R_{max}} \right) \rceil$, we obtain
 952

$$\text{Bias}(\mathcal{L}_{group}(k)) \leq \epsilon = \min\{\text{Bias}(\mathcal{L}_{traj}), \text{Bias}(\mathcal{L}_{step})\} + \epsilon. \quad (28)$$

972 Next, we analyze the variance of the three losses. We derive element-wise bounds on the variance
 973 of the empirical loss
 974

$$975 \mathcal{L}_\bullet = \frac{1}{|\mathcal{D}_\bullet|} \sum_{(u_w, u_l) \in \mathcal{D}_\bullet} \ell(\Delta_\theta), \quad \ell(\Delta_\theta) := -\log \sigma(\beta \Delta_\theta), \quad (29)$$

977 for $\bullet \in \{\text{traj, step, group}\}$. All samples are generated from N i.i.d. trajectories.
 978

979 For trajectory-level DPO, each trajectory contributes exactly one preference pair. The total number
 980 of samples $|\mathcal{D}_{\text{traj}}| = N$. The N pairs are i.i.d., hence the covariance terms in the variance vanish:
 981

$$982 \text{Var}(\mathcal{L}_{\text{traj}}) = \frac{1}{N^2} \sum_{i=1}^N \text{Var} \left[\ell(\Delta_\theta^{(i)}) \right] = \frac{1}{N} \Sigma_{\text{traj}}, \quad (30)$$

984 where $\Sigma_{\text{traj}} := \text{Var}[\ell(\Delta_\theta)]$ under the trajectory-level sampling distribution.
 985

986 For step-level DPO, from one trajectory we extract T consecutive suffixes $(u_t)_{t=1}^T$ with $u_t =$
 987 (s_t, \dots, s_T) . The total number of samples is $|\mathcal{D}_{\text{step}}| = NT$. However, the T samples inside
 988 one trajectory are highly overlapped. Sequence u_t and u_{t+1} share $T - t - 1$ identical transitions.
 989 Therefore the covariance part in covariance is non-zero and large.
 990

991 Since $|\Delta_\theta| \leq \frac{2R_{\max}}{1-\gamma}$, we have $0 \leq \ell(\Delta_\theta) \leq L_{\max} := \log(1 + e^{\frac{2\beta R_{\max}}{1-\gamma}})$. For any $t < s \leq T$, let
 992 $o = s - t$ (number of shared steps). The Cauchy-Schwarz inequality gives $\text{Cov}(\ell_t, \ell_s) \leq \gamma^o L_{\max}^2$.
 993 Summing over ordered pairs in one trajectory, we get
 994

$$995 \sum_{1 \leq t < s \leq T} \text{Cov}(\ell_t, \ell_s) \leq L_{\max}^2 \sum_{o=1}^{T-1} (T - o) \gamma^o < L_{\max}^2 \frac{\gamma}{(1 - \gamma)^2}. \quad (31)$$

997 We now consider total variance across N trajectories. Each trajectory contributes T samples, and
 998 samples from different trajectories are i.i.d. Hence,
 999

$$1000 \text{Var}(\mathcal{L}_{\text{step}}) = \frac{1}{(NT)^2} \left[N \cdot T \cdot \text{Var}(\ell_t) + N \cdot 2 \sum_{1 \leq t < s \leq T} \text{Cov}(\ell_t, \ell_s) \right] \quad (32)$$

$$1003 \leq \frac{L_{\max}^2}{NT} + \frac{2L_{\max}^2 \gamma}{NT(1 - \gamma)^2} = \frac{L_{\max}^2}{NT} \left(1 + \frac{2\gamma}{(1 - \gamma)^2} \right). \quad (33)$$

1005 $\text{Var}(\mathcal{L}_{\text{step}})$ is $O(\frac{1}{NT})$ but with a constant that does not degrade with T .
 1006

1007 For group-level DPO, we extract $M = \lfloor T/k \rfloor$ non-overlapping groups of length k . The total num-
 1008 ber of samples is $|\mathcal{D}_{\text{group}}| = NM$. Between-trajectory samples are i.i.d., while within-trajectory
 1009 samples are independent by construction. Therefore, the covariance terms in variance are zero, and
 1010

$$1011 \text{Var}(\mathcal{L}_{\text{group}}(k)) = \frac{1}{(NM)^2} \cdot NM \cdot \text{Var}[\ell(\Delta_\theta)] = \frac{1}{NM} \Sigma_{\text{group}}, \quad (34)$$

1012 where $\Sigma_{\text{group}} := \text{Var}[\ell(\Delta_\theta)]$ under the group-level distribution. Since a sub-trajectory has smaller
 1013 variance than the full trajectory, $\Sigma_{\text{group}} \leq \Sigma_{\text{traj}}$. Inserting $M \geq T/k - 1$ into Equation 34, we
 1014 obtain
 1015

$$1016 \text{Var}(\mathcal{L}_{\text{group}}(k)) \leq \frac{k}{T} \cdot \frac{1}{N} \Sigma_{\text{traj}} = \frac{k}{T} \text{Var}(\mathcal{L}_{\text{traj}}). \quad (35)$$

1017 An identical comparison with step-DPO gives
 1018

$$1019 \text{Var}(\mathcal{L}_{\text{group}}(k)) \leq \frac{Ck}{T} \text{Var}(\mathcal{L}_{\text{step}}), \quad C = \frac{2\text{tr}(\Sigma_{\text{step}})}{\text{tr}(\Sigma_{\text{group}})} \geq 1. \quad (36)$$

1020 The constant C depends only on γ and R_{\max} , and is independent of T, k , and N .
 1021

1022 With $k(\epsilon) = \lceil \log_\gamma \left(\frac{(1-\gamma)\epsilon}{2\beta R_{\max}} \right) \rceil = \Theta(\log(1/\epsilon))$, Equation 35 and 36 yield
 1023

$$1024 \text{Var}(\mathcal{L}_{\text{group}}(k)) \leq \frac{C \log(1/\epsilon)}{T} \min\{\text{Var}(\mathcal{L}_{\text{traj}}), \text{Var}(\mathcal{L}_{\text{step}})\}, \quad (37)$$

1025 which is the variance bound claimed in the proposition. \square

1026 G ADDITIONAL EXPERIMENTS

1029 G.1 SUB-TASK PERFORMANCE ON ALFWORLD

1031 To provide a more fine-grained analysis of our method’s capabilities, we present a detailed break-
 1032 down of success rates on the six distinct sub-task types in ALFWORLD for both seen (Table 6) and
 1033 unseen (Table 7) sets. The largest performance gains are often observed in the complex sub-tasks,
 1034 such as Examine and Pick2, which require longer reasoning chains.

1035 Table 6: Sub-task success rate (%) comparison on the ALFWORLD seen set.

1038 1039 1040 1041 1042 1043 1044 1045 1046 1047 1048 1049 1050 1051 1052 1053 1054 1055 1056 1057 1058 1059 1060 1061 1062 1063 1064 1065 1066 1067 1068 1069 1070 1071 1072 1073 1074 1075 1076 1077 1078 1079 1080 1081 1082 1083 1084 1085 1086 1087 1088 1089 1090 1091 1092 1093 1094 1095 1096 1097 1098 1099 1100 1101 1102 1103 1104 1105 1106 1107 1108 1109 1110 1111 1112 1113 1114 1115 1116 1117 1118 1119 1120 1121 1122 1123 1124 1125 1126 1127 1128 1129 1130 1131 1132 1133 1134 1135 1136 1137 1138 1139 1140 1141 1142 1143 1144 1145 1146 1147 1148 1149 1150 1151 1152 1153 1154 1155 1156 1157 1158 1159 1160 1161 1162 1163 1164 1165 1166 1167 1168 1169 1170 1171 1172 1173 1174 1175 1176 1177 1178 1179 1180 1181 1182 1183 1184 1185 1186 1187 1188 1189 1190 1191 1192 1193 1194 1195 1196 1197 1198 1199 1200 1201 1202 1203 1204 1205 1206 1207 1208 1209 1210 1211 1212 1213 1214 1215 1216 1217 1218 1219 1220 1221 1222 1223 1224 1225 1226 1227 1228 1229 1230 1231 1232 1233 1234 1235 1236 1237 1238 1239 1240 1241 1242 1243 1244 1245 1246 1247 1248 1249 1250 1251 1252 1253 1254 1255 1256 1257 1258 1259 1260 1261 1262 1263 1264 1265 1266 1267 1268 1269 1270 1271 1272 1273 1274 1275 1276 1277 1278 1279 1280 1281 1282 1283 1284 1285 1286 1287 1288 1289 1290 1291 1292 1293 1294 1295 1296 1297 1298 1299 1300 1301 1302 1303 1304 1305 1306 1307 1308 1309 1310 1311 1312 1313 1314 1315 1316 1317 1318 1319 1320 1321 1322 1323 1324 1325 1326 1327 1328 1329 1330 1331 1332 1333 1334 1335 1336 1337 1338 1339 1340 1341 1342 1343 1344 1345 1346 1347 1348 1349 1350 1351 1352 1353 1354 1355 1356 1357 1358 1359 1360 1361 1362 1363 1364 1365 1366 1367 1368 1369 1370 1371 1372 1373 1374 1375 1376 1377 1378 1379 1380 1381 1382 1383 1384 1385 1386 1387 1388 1389 1390 1391 1392 1393 1394 1395 1396 1397 1398 1399 1400 1401 1402 1403 1404 1405 1406 1407 1408 1409 1410 1411 1412 1413 1414 1415 1416 1417 1418 1419 1420 1421 1422 1423 1424 1425 1426 1427 1428 1429 1430 1431 1432 1433 1434 1435 1436 1437 1438 1439 1440 1441 1442 1443 1444 1445 1446 1447 1448 1449 1450 1451 1452 1453 1454 1455 1456 1457 1458 1459 1460 1461 1462 1463 1464 1465 1466 1467 1468 1469 1470 1471 1472 1473 1474 1475 1476 1477 1478 1479 1480 1481 1482 1483 1484 1485 1486 1487 1488 1489 1490 1491 1492 1493 1494 1495 1496 1497 1498 1499 1500 1501 1502 1503 1504 1505 1506 1507 1508 1509 1510 1511 1512 1513 1514 1515 1516 1517 1518 1519 1520 1521 1522 1523 1524 1525 1526 1527 1528 1529 1530 1531 1532 1533 1534 1535 1536 1537 1538 1539 1540 1541 1542 1543 1544 1545 1546 1547 1548 1549 1550 1551 1552 1553 1554 1555 1556 1557 1558 1559 1560 1561 1562 1563 1564 1565 1566 1567 1568 1569 1570 1571 1572 1573 1574 1575 1576 1577 1578 1579 1580 1581 1582 1583 1584 1585 1586 1587 1588 1589 1590 1591 1592 1593 1594 1595 1596 1597 1598 1599 1599 1600 1601 1602 1603 1604 1605 1606 1607 1608 1609 1610 1611 1612 1613 1614 1615 1616 1617 1618 1619 1620 1621 1622 1623 1624 1625 1626 1627 1628 1629 1630 1631 1632 1633 1634 1635 1636 1637 1638 1639 1640 1641 1642 1643 1644 1645 1646 1647 1648 1649 1650 1651 1652 1653 1654 1655 1656 1657 1658 1659 1660 1661 1662 1663 1664 1665 1666 1667 1668 1669 1670 1671 1672 1673 1674 1675 1676 1677 1678 1679 1680 1681 1682 1683 1684 1685 1686 1687 1688 1689 1690 1691 1692 1693 1694 1695 1696 1697 1698 1699 1700 1701 1702 1703 1704 1705 1706 1707 1708 1709 17010 17011 17012 17013 17014 17015 17016 17017 17018 17019 17020 17021 17022 17023 17024 17025 17026 17027 17028 17029 17030 17031 17032 17033 17034 17035 17036 17037 17038 17039 17040 17041 17042 17043 17044 17045 17046 17047 17048 17049 17050 17051 17052 17053 17054 17055 17056 17057 17058 17059 17060 17061 17062 17063 17064 17065 17066 17067 17068 17069 17070 17071 17072 17073 17074 17075 17076 17077 17078 17079 17080 17081 17082 17083 17084 17085 17086 17087 17088 17089 17090 17091 17092 17093 17094 17095 17096 17097 17098 17099 170100 170101 170102 170103 170104 170105 170106 170107 170108 170109 170110 170111 170112 170113 170114 170115 170116 170117 170118 170119 170120 170121 170122 170123 170124 170125 170126 170127 170128 170129 170130 170131 170132 170133 170134 170135 170136 170137 170138 170139 170140 170141 170142 170143 170144 170145 170146 170147 170148 170149 170150 170151 170152 170153 170154 170155 170156 170157 170158 170159 170160 170161 170162 170163 170164 170165 170166 170167 170168 170169 170170 170171 170172 170173 170174 170175 170176 170177 170178 170179 170180 170181 170182 170183 170184 170185 170186 170187 170188 170189 170190 170191 170192 170193 170194 170195 170196 170197 170198 170199 170200 170201 170202 170203 170204 170205 170206 170207 170208 170209 170210 170211 170212 170213 170214 170215 170216 170217 170218 170219 170220 170221 170222 170223 170224 170225 170226 170227 170228 170229 170230 170231 170232 170233 170234 170235 170236 170237 170238 170239 170240 170241 170242 170243 170244 170245 170246 170247 170248 170249 170250 170251 170252 170253 170254 170255 170256 170257 170258 170259 170260 170261 170262 170263 170264 170265 170266 170267 170268 170269 170270 170271 170272 170273 170274 170275 170276 170277 170278 170279 170280 170281 170282 170283 170284 170285 170286 170287 170288 170289 170290 170291 170292 170293 170294 170295 170296 170297 170298 170299 170299 170300 170301 170302 170303 170304 170305 170306 170307 170308 170309 170310 170311 170312 170313 170314 170315 170316 170317 170318 170319 170320 170321 170322 170323 170324 170325 170326 170327 170328 170329 170330 170331 170332 170333 170334 170335 170336 170337 170338 170339 170340 170341 170342 170343 170344 170345 170346 170347 170348 170349 170350 170351 170352 170353 170354 170355 170356 170357 170358 170359 170360 170361 170362 170363 170364 170365 170366 170367 170368 170369 170370 170371 170372 170373 170374 170375 170376 170377 170378 170379 170380 170381 170382 170383 170384 170385 170386 170387 170388 170389 170390 170391 170392 170393 170394 170395 170396 170397 170398 170399 170399 170400 170401 170402 170403 170404 170405 170406 170407 170408 170409 170410 170411 170412 170413 170414 170415 170416 170417 170418 170419 170420 170421 170422 170423 170424 170425 170426 170427 170428 170429 170430 170431 170432 170433 170434 170435 170436 170437 170438 170439 170440 170441 170442 170443 170444 170445 170446 170447 170448 170449 170450 170451 170452 170453 170454 170455 170456 170457 170458 170459 170460 170461 170462 170463 170464 170465 170466 170467 170468 170469 170470 170471 170472 170473 170474 170475 170476 170477 170478 170479 170480 170481 170482 170483 170484 170485 170486 170487 170488 170489 170490 170491 170492 170493 170494 170495 170496 170497 170498 170499 170499 170500 170501 170502 170503 170504 170505 170506 170507 170508 170509 170510 170511 170512 170513 170514 170515 170516 170517 170518 170519 170520 170521 170522 170523 170524 170525 170526 170527 170528 170529 170530 170531 170532 170533 170534 170535 170536 170537 170538 170539 170540 170541 170542 170543 170544 170545 170546 170547 170548 170549 170550 170551 170552 170553 170554 170555 170556 170557 170558 170559 170560 170561 170562 170563 170564 170565 170566 170567 170568 170569 170570 170571 170572 170573 170574 170575 170576 170577 170578 170579 170580 170581 170582 170583 170584 170585 170586 170587 170588 170589 170590 170591 170592 170593 170594 170595 170596 170597 170598 170599 170599 170600 170601 170602 170603 170604 170605 170606 170607 170608 170609 170610 170611 170612 170613 170614 170615 170616 170617 170618 170619 170620 170621 170622 170623 170624 170625 170626 170627 170628 170629 170630 170631 170632 170633 170634 170635 170636 170637 170638 170639 170640 170641 170642 170643 170644 170645 170646 170647 170648 170649 170650 170651 170652 170653 170654 170655 170656 170657 170658 170659 170660 170661 170662 170663 170664 170665 170666 170667 170668 170669 170670 170671 170672 170673 170674 170675 170676 170677 170678 170679 170680 170681 170682 170683 170684 170685 170686 170687 170688 170689 170690 170691 170692 170693 170694 170695 170696 170697 170698 170699 170699 170700 170701 170702 170703 170704 170705 170706 170707 170708 170709 170710 170711 170712 170713 170714 170715 170716 170717 170718 170719 170720 170721 170722 170723 170724 170725 170726 170727 170728 170729 170730 170731 170732 170733 170734 170735 170736 170737 170738 170739 170740 170741 170742 170743 170744 170745 170746 170747 170748 170749 170750 170751 170752 170753 170754 170755 170756 170757 170758 170759 170760 170761 170762 170763 170764 170765 170766 170767 170768 170769 170770 170771 170772 170773 170774 170775 170776 170777 170778 170779 170780 170781 170782 170783 170784 170785 170786 170787 170788 170789 170790 170791 170792 170793 170794 170795 170796 170797 170798 170799 170799 170800 170801 170802 170803 170804 170805 170806 170807 170808 170809 170810 170811 170812 170813 170814 170815 170816 170817 170818 170819 170820 170821 170822 170823 170824 170825 170826 170827 170828 170829 170830 170831 170832 170833 170834 170835 170836 170837 170838 170839 170840 170841 170842 170843 170844 170845 170846 170847 170848 170849 170850 170851 170852 170853 170854 170855 170856 170857 170858 170859 170860 170861 170862 170863 170864 170865 170866 170867 170868 170869 170870 170871 170872 170873 170874 170875 170876 170877 170878 170879 170880 170881 170882 170883 170884 170885 170886

1080 G.2 CASE STUDY
10811082 G.2.1 ALFWORLD
10831084 Case Study of ALFWorld
10851086 IPR
1087

Task Instruction: You are in the middle of a room. Looking quickly around you, you see a cabinet 6, a cabinet 5, a cabinet 4, a cabinet 3, a cabinet 2, a cabinet 1, a coffeemachine 1, a countertop 3, a countertop 2, a countertop 1, a drawer 3, a drawer 2, a drawer 1, a fridge 1, a garbagecan 1, a microwave 1, a shelf 3, a shelf 2, a shelf 1, a sinkbasin 1, a stoveburner 4, a stoveburner 3, a stoveburner 2, a stoveburner 1, and a toaster 1.

Your task is to: put a cool mug in cabinet.

Thought: I need to find a mug to put in the cabinet. The task description doesn't specify where the mug is, so I should look around the room to locate one.

Action: go to toaster 1

Observation: On the toaster 1, you see nothing.

Thought: The toaster is not where mugs would typically be found, but it's good to check all areas systematically. There's nothing on the toaster, so I'll continue searching.

Action: go to stoveburner 1

Observation: On the stoveburner 1, you see a pot 1.

..... (search for the mug)

Thought: Cabinet 3 has a vase, but no mug. I'll check cabinet 4.

Action: go to cabinet 4

Observation: On the cabinet 4, you see a mug 2.

Thought: Cabinet 4 has a mug. This could be the mug I need to put in the cabinet. I'll take it and then place it in the cabinet.

Action: take mug 2 from cabinet 4

Observation: You pick up the mug 2 from the cabinet 4.

Thought: With the mug in hand, I need to return to cabinet 1 to place the mug inside.

Action: go to cabinet 1

Observation: On the cabinet 1, you see a peppershaker 1, a soapbottle 1, and a vase 2.

Thought: To complete the task, I need to put the mug into the cabinet.

Action: put mug 2 in/on cabinet 1

Observation: You put the mug 2 in/on the cabinet 1.

1086 HPL
1087

Task Instruction: You are in the middle of a room. Looking quickly around you, you see a cabinet 6, a cabinet 5, a cabinet 4, a cabinet 3, a cabinet 2, a cabinet 1, a coffeemachine 1, a countertop 3, a countertop 2, a countertop 1, a drawer 3, a drawer 2, a drawer 1, a fridge 1, a garbagecan 1, a microwave 1, a shelf 3, a shelf 2, a shelf 1, a sinkbasin 1, a stoveburner 4, a stoveburner 3, a stoveburner 2, a stoveburner 1, and a toaster 1.

Your task is to: put a cool mug in cabinet.

Thought: I need to find a mug to put in the cabinet. The sink basin is a common place where mugs are found after being used or washed.

Action: go to sinkbasin 1

Observation: On the sinkbasin 1, you see a cup 1, a dishponge 2, a plate 2, and a potato 1.

Thought: There is no mug at the sink basin, but there are other items here. I should check the shelves as they often store mugs.

Action: go to shelf 1

Observation: On the shelf 1, you see a creditcard 3.

..... (search for the mug)

Thought: Cabinet 3 has a vase but no mug. I'll proceed to the next cabinet.

Action: go to cabinet 4

Observation: On the cabinet 4, you see a mug 2.

Thought: I found a mug in cabinet 4. I need to take it so I can put it in the cooler as instructed.

Action: take mug 2 from cabinet 4

Observation: You pick up the mug 2 from the cabinet 4.

Thought: Now that I have the mug, I need to cool it. The fridge is the best place to do this.

Action: go to fridge 1

Observation: The fridge 1 is closed.

Thought: The fridge is closed. I need to open it to cool the mug.

Action: cool mug 2 with fridge 1

Observation: You cool the mug 2 using the fridge 1.

1134	# The agent mistakenly believes that the task	
1135	has been completed.	
1136		Thought: The mug is now cool. I should return to the cabinet to complete the task.
1137	Thought: The task is now complete, and I	Action: go to cabinet 1
1138	should prepare to move on to the next task or	Observation: On the cabinet 1, you see a
1139	task set. I need to ensure that I approach each	peppershaker 1, a soapbottle 1, and a vase 2.
1140	task with clarity and precision, adhering to	Thought: I am back at cabinet 1. I need to
1141	the given instructions and using the appropriate	put the cool mug in the cabinet as per the task
1142	tools and resources.	instructions.
1143	Action: prepare for next task	Action: put mug 2 in/on cabinet 1
1144	Observation: Nothing happens.	Reward: 1.0
1145 (until the steps are exhausted)	
1146	Reward: 0.0	
1147		
1148		
1149		
1150		
1151	G.2.2 WEBSHOP	
1152		
1153	Case Study of WebShop	
1154		
1155		
1156		
1157		
1158		
1159		
1160		
1161		
1162		
1163		
1164		
1165		
1166		
1167		
1168		
1169		
1170		
1171		
1172		
1173		
1174		
1175		
1176		
1177		
1178		
1179		
1180		
1181		
1182		
1183		
1184		
1185		
1186		
1187		
1188		

G.2.2 WEBSHOP

Case Study of WebShop

IPR

Task Instruction: I am looking for a gluten free, 100% vegan plant based protein shake that is soy-free, and price lower than 40.00 dollars.

Thought: I need to find a plant-based protein shake that meets specific criteria including being gluten-free, 100% vegan, soy-free, and under \$40. I'll start by searching with these details.

Action: search[gluten free, 100% vegan plant based protein shake that is soy-free]

Observation: Page 1 (Total results: 50) [SEP] Next > [SEP] B08FW5Y13G [SEP] Orgain Bundle - Chocolate and Vanilla Bean Protein Powder - ... [SEP] \$53.98 [SEP] B0885Y2GD4 [SEP] OWYN 100% Vegan Plant-Based Protein Shake, Cookies & Creamless, 1 Count, with 20g Plant Protein, ... [SEP] \$100.00 (other product details)

Thought: The first page of results doesn't seem to have any options that fit all my criteria. I should check the next page for more options.

Action: click[next >]

Observation: Page 2 (Total results: 50) [SEP] < Prev [SEP] Next > [SEP] B07DM8SP27 [SEP] OWYN 100% Vegan Plant-Based Protein Shake, Strawberry Banana, 24 Pack, 20g Plant Protein ... [SEP] \$71.18 [SEP] B08H8VJGZ [SEP] OWYN - 100% Vegan Plant-Based Pro Elite High Protein Shakes | Vanilla, 12 Fl Oz ... [SEP] \$4.48 [SEP] (other product details)

HPL

Task Instruction: I am looking for a gluten free, 100% vegan plant based protein shake that is soy-free, and price lower than 40.00 dollars.

Thought: I need to find a plant-based protein shake that meets specific criteria including being gluten-free, 100% vegan, soy-free, and under \$40. I'll start by searching with these details.

Action: search[gluten free, 100% vegan plant based protein shake that is soy-free]

Observation: Page 1 (Total results: 50) [SEP] Next > [SEP] B08FW5Y13G [SEP] Orgain Bundle - Chocolate and Vanilla Bean Protein Powder - ... [SEP] \$53.98 [SEP] B0885Y2GD4 [SEP] OWYN 100% Vegan Plant-Based Protein Shake, Cookies & Creamless, 1 Count, with 20g Plant Protein, ... [SEP] \$100.00 (other product details)

Thought: The first page of results doesn't seem to have any options that fit all my criteria. I should check the next page for more options.

Action: click[next >]

Observation: Page 2 (Total results: 50) [SEP] < Prev [SEP] Next > [SEP] B07DM8SP27 [SEP] OWYN 100% Vegan Plant-Based Protein Shake, Strawberry Banana, 24 Pack, 20g Plant Protein ... [SEP] \$71.18 [SEP] B08H8VJGZ [SEP] OWYN - 100% Vegan Plant-Based Pro Elite High Protein Shakes | Vanilla, 12 Fl Oz ... [SEP] \$4.48 [SEP] (other product details)

1188

1189

1190

1191

1192

1193

1194

1195

1196

1197

1198

1199

1200

1201

1202

1203

1204

1205

1206

1207

1208

1209

1210

1211

1212

1213

1214

1215

1216

1217

Thought: On the second page, I see a product called “OWYN 100% Vegan Plant-Based Protein Shake” which seems to match most of my requirements except for the price. It’s also listed as soy-free and vegan, and it’s well below \$40. I’ll take a closer look at this option.

Action: click[b07dm8sp27]

Observation: < Prev [SEP] OWYN 100% Vegan Plant-Based Protein Shake, Strawberry Banana, 24 Pack, 20g Plant Protein with Omega-3, Prebiotic supplements, Superfoods Greens Blend, Gluten-Free, Soy-Free, Non-GMO [SEP] Price: \$71.18 [SEP] Rating: [SEP] Description [SEP] Features [SEP] Reviews [SEP] Buy Now

Thought: This product has a high price compared to my budget, and although it’s described as vegan and soy-free, the price is above \$40. Since I’m looking for something within my budget, I might reconsider or look for another option that fits all my criteria including the price limit.

Action: click[buy now]

Reward: 0.5

Thought: On the second page, I see a product called “OWYN 100% Vegan Plant-Based Protein Shake” which seems to match my requirements. It’s also well within my budget at \$4.48. I should take a closer look at this option.

Action: click[b08h8vjjgz]

Observation: < Prev [SEP] OWYN - 100% Vegan Plant-Based Pro Elite High Protein Shakes | Vanilla, 12 Fl Oz | Dairy-Free, Gluten-Free, Soy Free, Keto Friendly, Zero Sugar, Vegetarian [SEP] Price: \$4.48 [SEP] Rating: [SEP] Description [SEP] Features [SEP] Reviews [SEP] Buy Now

Thought: This product has all the features I’m looking for.

Action: click[buy now]

Reward: 1.0

G.2.3 INTERCODE-SQL

Case Study of InterCode-SQL

IPR

Task Instruction: What is the money rank of the tallest poker player?

Thought: I need to check what tables are available to use.

Action: SHOW TABLES

Observation: [(‘people’,), (‘poker_player’,)]

Thought: There are two tables available, ‘people’ and ‘poker_player’. Since the question is asking about the money rank of the tallest poker player, I should check if there is a table related to poker players.

Action: DESC poker_player

Observation: [(‘Poker_Player_ID’, ‘int’, ‘NO’, ‘PRI’, None, ‘auto_increment’), (‘People_ID’, ‘int’, ‘YES’, ‘MUL’, None, ‘’), (‘Final_Table_Made’, ‘double’, ‘YES’, ‘’, None, ‘’), (‘Best_Finish’, ‘double’, ‘YES’, ‘’, None, ‘’), (‘Money_Rank’, ‘double’, ‘YES’, ‘’, None, ‘’), (‘Earnings’, ‘double’, ‘YES’, ‘’, None, ‘’)]

HPL

Task Instruction: What is the money rank of the tallest poker player?

Thought: I need to check what tables are available to use.

Action: SHOW TABLES

Observation: [(‘people’,), (‘poker_player’,)]

Thought: The table ‘poker_player’ might have information about the height and money rank of the players. I should check the structure of this table.

Action: DESC poker_player

Observation: [(‘Poker_Player_ID’, ‘int’, ‘NO’, ‘PRI’, None, ‘auto_increment’), (‘People_ID’, ‘int’, ‘YES’, ‘MUL’, None, ‘’), (‘Final_Table_Made’, ‘double’, ‘YES’, ‘’, None, ‘’), (‘Best_Finish’, ‘double’, ‘YES’, ‘’, None, ‘’), (‘Money_Rank’, ‘double’, ‘YES’, ‘’, None, ‘’), (‘Earnings’, ‘double’, ‘YES’, ‘’, None, ‘’)]

1242
 1243
 1244
 1245
 1246
 1247
 1248
 1249
 1250
 1251
 1252
 1253
 1254
 1255
 1256
 1257
 1258
 1259
 1260
 1261
 1262
 1263
 1264
 1265
 1266
 1267
 1268
 1269
 1270
 1271
 1272
 1273
 1274
 1275
 1276
 1277
 1278
 1279
 1280
 1281
 1282
 1283
 1284
 1285
 1286
 1287
 1288
 1289
 1290
 1291
 1292
 1293
 1294
 1295

Thought: The ‘poker_player’ table contains information about poker players, including their money rank. To find the money rank of the tallest poker player, I need to join the ‘people’ table with the ‘poker_player’ table on the ‘People_ID’ column. Then, I can order the results based on height and limit the result to 1 to get the tallest poker player’s money rank.

Action:

```
SELECT Money_Rank
FROM people
JOIN poker_player ON
people.People_ID =
poker_player.Poker_Player_ID
ORDER BY height
LIMIT 1
```

Observation: [(141.0,)]

Thought: The query executed successfully and returned a single number, which is the money rank of the tallest poker player. This should be the answer to the question.

Action: submit

Reward: 0.0

Thought: The ‘poker_player’ table contains columns for money rank and height. I can write a SQL query to find the money rank of the tallest poker player.

Action:

Observation: Error executing query: Unknown column ‘Height’ in ‘order clause’.

Thought: Oops, it seems like there is no column named ‘Height’ in the ‘poker_player’ table. I should check the structure of the ‘people’ table to see if it has the height information.

Action: DESC people

Observation: [(‘People_ID’, ‘int’, ‘NO’, ‘PRI’, None, ‘auto_increment’), (‘Nationality’, ‘text’, ‘YES’, ‘’, None, ‘’), (‘Name’, ‘text’, ‘YES’, ‘’, None, ‘’), (‘Birth_Date’, ‘text’, ‘YES’, ‘’, None, ‘’), (‘Height’, ‘double’, ‘YES’, ‘’, None, ‘’)]

Thought: The ‘people’ table does have a column for height. I can join the ‘poker_player’ and ‘people’ tables to get the money rank of the tallest poker player.

Action:

Observation: [(68.0,)]

Thought: The query executed successfully and returned the money rank of the tallest poker player as 68. This should be the answer to the question.

Action: submit

Reward: 1.0

H PROMPTS

H.1 ALFWORLD

Instruction Prompt for ALFWorld

Interact with a household to solve a task. Imagine you are an intelligent agent in a household environment and your target is to perform actions to complete the task goal. At the beginning of your interactions, you will be given the detailed description of the current environment and your goal to accomplish.

1296
 1297 For each of your turn, you will be given the observation of the last turn. You should first think
 1298 about the current condition and plan for your future actions, and then output your action in
 1299 this turn. Your output must strictly follow this format: "Thought: your thoughts.\nAction:
 1300 your next action".
 1301

1301 The available actions are:

1. go to {recep}
2. take {obj} from {recep}
3. put {obj} in/on {recep}
4. open {recep}
5. close {recep}
6. toggle {obj} {recep}
7. clean {obj} with {recep}
8. heat {obj} with {recep}
9. cool {obj} with {recep}

1313 where {obj} and {recep} correspond to objects and receptacles.
 1314

1315 After your each turn, the environment will give you immediate feedback based on which
 1316 you plan your next few steps. if the environment output "Nothing happened", that means the
 1317 previous action is invalid and you should try more options.
 1318

1319 Your response should use the following format:
 1320 Thought: <your thoughts>
 1321 Action: <your next action>
 1322

Semantic Grouping Prompt for ALFWorld

1325 I need you to help me divide the trajectory of an agent's interaction with the environment into
 1326 multiple action groups based on semantic relevance.
 1327

1328 Below is an interaction trajectory, which contains the environment description received by
 1329 the agent and the sequence of actions performed:
 1330 {trajectory}

1331 Please divide the action sequence in this trajectory into multiple semantically related groups,
 1332 each group represents a set of actions to complete a sub-goal or sub-task.
 1333

1334 Please follow the following principles when dividing:
 1335

1. Actions in the same group should be semantically closely related and complete a clear subtask together
2. When the purpose of an action changes, it should be divided into a new group
3. For each group, briefly describe the common goal of the group of actions

1339 Please use the following format to return the results:
 1340

1341 <action_groups>

1342 Group 1 (action index: 0-2): Find the target item

1343 - Action 0: go to toiletpaperhanger 1

1344 - Action 1: go to toilet 1

1345 - Action 2: take toiletpaper 1 from toilet 1

1346 Group 2 (action index: 3-4): Complete the main task

1347 - Action 3: go to toiletpaperhanger 1

1348 - Action 4: put toiletpaper 1 in/on toiletpaperhanger 1

1349 </action_groups>

1350
1351

H.2 WEBSHOP

1352
1353

Instruction Prompt for WebShop

1354

You are web shopping.

1355

I will give you instructions about what to do.

1356

You have to follow the instructions.

1357

Every round I will give you an observation and a list of available actions, you have to respond an action based on the state and instruction.

1358

You can use search action if search is available.

1359

You can click one of the buttons in clickables.

1360

1361

You are web shopping.

1362

An action should be of the following structure:

1363

search[keywords]

1364

click[value]

1365

1366

If the action is not valid, perform nothing.

1367

Keywords in search are up to you, but the value in click must be a value in the list of available

1368

actions.

1369

Remember that your keywords in search should be carefully designed.

1370

1371

Your response should use the following format:

1372

Thought: I think ...

1373

Action: click[something]

1374

1375

Semantic Grouping Prompt for WebShop

1376

1377

I need you to divide a sequence of actions into groups based on semantic relevance.

1378

1379

A possible grouping example:

1380

1381

Group 1 (action index: 0-0): Initial search phase

1382

- Action 0: search[size 5 patent-beige high heel]

1383

1384

Group 2 (action index: 1-1): Preliminary screening and click to view product details

1385

- Action 1: click[b09gxnyjcd]

1386

1387

Group 3 (action index: 2-3): Specification confirmation and detailed screening stage

1388

- Action 2: click[beige-almond toe-patent leather]

1389

- Action 3: click[5]

1390

1391

Group 4 (action index: 4-4): Purchase decision stage

1392

- Action 4: click[buy now]

1393

1394

Your output then should be in the following format:

1395

[[0, 0], [1, 1], [2, 3], [4, 4]]

1396

1397

Below is the interaction trajectory:

{trajectory}

1398

1399

Please group the actions by their indices. Your response MUST be a valid JSON array of arrays of integers, where each inner array represents a group of action indices.

1400

1401

1402

1403

Follow these rules STRICTLY:

1. Each action must belong to exactly one group.

2. The indices must be contiguous and cover the entire range from 0 to {num_actions} - 1.

1404
 1405 3. The final output MUST NOT contain any text, explanations, code blocks, or markdown
 1406 formatting outside of the JSON array itself. It should be a raw JSON string.
 1407 4. The last number in the last group MUST be $\{ \text{num_actions} \} - 1$.
 1408
 1409 Example for a trajectory with 5 actions (indices 0, 1, 2, 3, 4):
 1410 $[[0, 1], [2, 3], [4, 4]]$
 1411
 1412 Another valid example:
 1413 $[[0, 0], [1, 2], [3, 4]]$
 1414
 1415 Your output must be only the JSON, like this:
 1416 $[[0, 1], [2, 3], [4, 4]]$

1417 H.3 INTERCODE-SQL

1420 Instruction Prompt for InterCode-SQL

1422 You are a helpful assistant assigned with the task of problem-solving. To achieve this, you
 1423 will interact with a MySQL Database system using SQL queries to answer a question.
 1424 At each turn, you should first provide your step-by-step thinking for solving the task. Your
 1425 thought process should start with “Thought: ”, for example: Thought: I should write a SQL
 1426 query that gets the average GNP and total population from nations whose government is US
 1427 territory.

1428 After that, you have two options:

1429 1) Interact with a mysql programming environment and receive the corresponding output.
 1430 Your code should start with “Action: ” and should be surrounded with ‘`sql`’ tag, for
 1431 example:

1432 Action:

1433 ‘`sql`
 1434 SELECT AVG(GNP), SUM(population)
 1435 FROM nations
 1436 WHERE government = ‘US Territory’;
 1437 ‘`’

1438 2) Directly submit the result, for example: Action: submit.

1439 You should use this format: “Thought: your thought\nAction: \n‘`sql`\n<the mysql
 1440 command>\n‘`’”. You will receive the corresponding output for your sql command.

1441 Your output should contain only one “Action” part.

1442 The “Action” part should be executed with a mysql interpreter or propose an answer. Any
 1443 natural language in it should be commented out.

1444 The SQL query and submit parts can not appear in your output simultaneously.

1448 Semantic Grouping Prompt for InterCode-SQL

1449 I need you to divide a sequence of actions into groups based on semantic relevance.

1450 A possible grouping example:

1451 Group 1 (action index: 0-1): Task initialization and data structure exploration phase

1452 - Action 0: SHOW TABLES

1453 - Action 1: DESC university

1458
1459 Group 2 (action index: 2-2): Query construction and execution phase
1460 - Action 2: SELECT Enrollment, Primary_conference FROM university
1461 ORDER BY Founded ASC LIMIT 1
1462
1463 Group 3 (action index: 3-3): Result confirmation and submission stage
1464 - Action 3: submit
1465
1466 Your output then should be in the following format:
1467 [[0, 1], [2, 2], [3, 3]]
1468
1469 Below is the interaction trajectory:
1470 {trajectory}
1471
1472 Please group the actions by their indices. Your response MUST be a valid JSON array of
1473 arrays of integers, where each inner array represents a group of action indices.
1474
1475 Follow these rules STRICTLY:
1476 1. Each action must belong to exactly one group.
1477 2. The indices must be contiguous and cover the entire range from 0 to {num_actions} - 1.
1478 3. The final output MUST NOT contain any text, explanations, code blocks, or markdown
1479 formatting outside of the JSON array itself. It should be a raw JSON string.
1480 4. The last number in the last group MUST be {num_actions} - 1.
1481
1482 Example for a trajectory with 5 actions (indices 0, 1, 2, 3, 4):
1483 [[0, 1], [2, 3], [4, 4]]
1484
1485 Another valid example:
1486 [[0, 0], [1, 2], [3, 4]]
1487
1488
1489
1490
1491
1492
1493
1494
1495
1496
1497
1498
1499
1500
1501
1502
1503
1504
1505
1506
1507
1508
1509
1510
1511